# Smart Beamforming for Direct Access to 5G-NR User Equipment from LEO Satellite at Ka-Band

**Author:**
Eduard Méndez López

**Supervisor:**
Prof. Ana Isabel Pérez Neira

Wireless Communications Specialization
Master's degree in Advanced Telecommunications Technologies

Escola Tècnica Superior d'Enginyeria de Telecomunicació de Barcelona
Universitat Politècnica de Catalunya

Signal Theory and Communications Departament
Universitat Politènica de Catalunya

August, 2020

# Abstract

Non-Terrestrial Networks (NTN), in particular LEO Satellite Networks, are expected to play a key role in extending and complementing terrestrial 5G networks in order to provide services to air, sea and un-served or under-served areas. This work proposes the implementation of a novel scheme called Resource Sharing Beamforming Access (RSBA), which seems a promising solution to deal with scenarios where Bit Error Rate (BER), probability of collision and/or achievable rate are important aspects of study. Given the system architecture presented in this work, RSBA will be proposed as solution in the 5G-NR Sat-IoT scenario. As it is expected, a huge amount of IoT devices will be transmitting in the uplink, and being the case of Non-Orthogonal-Multiple-Access (NOMA), the risk of collisions between devices will increase. The idea, after assessing the channel impairments of a direct link between a LEO Satellite and a NB-IoT device, it to study how spatial diversity via smart beamforming at the receiver will reduce the probability of collision between the devices, and thus increasing the number of users that can access to the media.

# Acknowledgements

First and foremost, I would like to thank my supervisor Ana Isabel Pérez Neira for her guidance and the knowledge that has provided me during these months. Despite the situation due to COVID-19, she has been supportive and has given me the opportunity to work in novel research.

Last, but nos least important, I would like to thank my parents and sister for the unceasing encouragement throughout this time at university.

# Acronyms

| | |
|---|---|
| **3GPP** | 3rd Generation Partnership Project |
| **4G LTE** | 4G Long Term Evolution |
| **5G NR** | 5G New Radio |
| **BER** | Bit Error Rate |
| **BLER** | Block Error Rate |
| **DMRS** | Demodulation Reference Signal |
| **DOA** | Direction of Arrival |
| **EFC** | Earth Fixed Coverage |
| **GNSS** | Global Navigation Satellite System |
| **IoT** | Internet-of-Things |
| **ITU** | International Telecommunication Union |
| **LEO** | Low-Earth-Orbit |
| **LOS** | Line-of-sight |
| **MIMO** | Multiple-Input Multiple-Output |
| **NB-IoT** | Narrowband-IoT |
| **NGSO** | Non-geostationary Orbit |
| **NOMA** | Non-Orthogonal Multiple Access |
| **NPRACH** | Narrowband Physical Random Access Channel |
| **NPUSCH** | Narrowband Physical Uplink Shared Channel |
| **NTN** | Non-Terrestrial Network |
| **OFDMA** | Orthogonal Frequency Division Multiple Access |
| **RDMA** | Repetition Division Multiple Access |
| **RSBA** | Resource Sharing Beamforming Access |
| **SC-FDMA** | Single Carrier Frequency Division Multiple Access |
| **SFC** | Satellite Fixed Coverage |
| **SNR** | Signal-to-Noise Ratio |
| **UE** | User Equipment |
| **eMBB** | Enhanced Mobile Broadband |
| **mMTC** | Massive Machine Type Communications |
| **uRLLC** | Ultra-reliable and Low-latency Communications |

# Contents

# List of Figures

# List of Tables

# Chapter 1

# Introduction

Nowadays, due to the high interest in 5G New Radio (5G NR) Non-Terrestrial Networks (NTN), the assessment of potential NR impacts to support NTN are currently under study [1]. It is expected that NR features may require some adaptations to support operation via Satellite (e.g. reference signals, cyclic prefix, sub-carrier spacing). 5G New Radio is the term used to refer to the new radio access technology standardized by 3GPP to meet the 5G requirements. Regarding 4G Long Term Evolution (4G LTE), some important features have been introduced with 5G NR.

Starting from the architectural point of view, the 5G system architecture has been devised to overcome LTE architecture limitations such as the impossibility of splitting parts of a functional entity (i.e. control and user plane) and place them at different locations, and the difficulties of optimizing or customizing the network to provide different behaviors for applications with different type of requirements (e.g. delay critical or bit rate demanding applications). Therefore, 5G NR provides a more modular design, instead of defining the architecture in terms of network entities, it specifies a set of Network Functions (NFs), facilitating the virtualization of the different NFs running on generic computer hardware. In addition to the split of control and user planes, one of the most important features that 5G NR architecture has introduced is the support of network slicing. In this way, one network can include the NFs to support mobile broadband services with full mobility support, and another one to support non-mobile, latency-critical industry applications.

Some of the main new characteristics of 5G NR in relation to 4G LTE are: the operation in higher frequency bands (up to 52.6 GHz) in addition to the usual bands below 6 GHz, the reduced amount of "always-on" signals, the forward compatibility with future technologies and applications, the low latency support in the order of 1 ms, and the extensive use of beamforming and massive multiple-input and multiple-output (MIMO). Moreover, it is expected that will meet large throughput increase (up to 20 Gbps in the downlink and 10 Gbps in the uplink), and reliability (99.999% of successful packet reception), amongst others [2].

The International Telecommunication Union (ITU) has classified 5G mobile network services into three different categories: Enhanced Mobile Broadband (eMBB), Ultra-reliable and Low-latency Communications (uRLLC), and Massive Machine Type Communications (mMTC). eMMB focuses on services that have high requirements for bandwidth, such as video streaming in high definition (HD), virtual reality (VR), and augmented reality (AR). These requirements will be fulfilled thanks to the possibility of having 5G bandwidths up to 400 MHz without employing carrier aggregation. The second category, uRLLC, focuses on latency-critical applications, such as autonomous and assisted driving, AR-assisted surgery, and factory industrial automation. Finally, being mMTC (or massive-IoT) the category related with this work, it aims to support high density scenarios, where hundreds of devices are transmitting simultaneously, using different or re-used resources.

## 1.1 Motivation

Mobile industry data researchers expect IoT connections to reach 25 billions by 2025, which is slightly more than the double of the 12 billions connections of 2019. Furthermore, despite the impact of the global coronavirus pandemic, IoT revenues will grow by 20% this year. Having hundreds or billions of IoT devices connected around the globe poses a significant operational challenge.

Today, the coverage provided by terrestrial networks only reaches 30% of the earth and 10% of the world. Furthermore, another important aspect regarding IoT devices is the security vulnerabilities. Thus, they need constant updates and future 5G devices will require an efficient distribution of data across the globe.

The wide coverage, the cost-effective implementation and the reliability that satellite communications provides stands out as a promising candidate to support IoT applications (e.g. industrial, agricultural and logistical applications). The role of NTN in 5G systems it is expected to be diverse, including: (i) extend and support the 5G service provision in un-served areas (e.g. isolated/remote areas, on board aircrafts or vessels) and under-served areas (e.g. sub-urban/rural areas); (ii) reinforce the 5G service reliability providing service continuity, in particular for critical communications, M2M/IoT devices or for passengers on board moving platforms (e.g. passenger vehicle-aircraft or ships); (iii) to enable the 5G network scalability by providing efficient multicast/broadcast resources for data delivery.

## 1.2 Problem Statement, Objectives and Contribution

Establishing a direct link between a user equipment (e.g. NB-IoT device) and a satellite poses several challenges. In fact, typical satellite channel impairments, such as large path losses, delays and Doppler shifts have to be assessed on the physical and Medium Access Control (MAC) layers.

In addition, the assessment of potential 5G NR impacts to support LEO Sat-IoT networks must be performed.

The work is focused on massive Machine Type Communications (mMTC) and, in particular, on a NB-IoT scenario at Ka-Band (20 GHz). One of the main advantages regarding the 20 GHz band is that there is no shared allocation with 5G Frequency Range 2 (FR2), which includes frequency bands from 24.25 GHz to 52.6 GHz. These bands have a shorter range but higher available bandwidth than the bands in the FR1 (i.e. frequency bands below 6 GHz). For mm-wave bands allocated to FR2 5G NR, the duplexing scheme foreseen is Time Division Duplexing (TDD), meaning that both uplink at downlink operations take place over the same frequency band and are separated only in the time domain. However, Frequency Division Duplexing (FDD) is assumed for core specification work for NR-NTN [3]. Note that this does not imply that TDD cannot be used for relevant scenarios (e.g. HAPS).

The contribution of this work aims to propose an alternative to the mode of massive access in the uplink employing a Non-Orthogonal Multiple Access (NOMA) strategy. The problem of providing massive connectivity with a limited satellite resources is solved by NOMA solutions. This non-orthogonal access allows the devices to use the same frequency/time resources and thus, achieve a higher spectral efficiency. Nevertheless, that requires to implement PHY-layer techniques, such as beamforming. As starting point, given the beam-centric paradigm of 5G NR at mm-waves, this work proposes an hybrid multibeamforming implementation at the LEO satellite. A recent study on direct access to 5G-NR UE from NGSO satellites [4] has investigated the feasibility of non-geostationary orbit (NGSO) satellites directly accessing NR-enabled User Equipment (UE) in mm-waves, from a regulatory, UE characteristics, space segment, link budget and system point of view. Despite the advancements in this new landscape, further investigations need to be carried on to complete the study. For example, improve the understanding of the regulatory landscape, how to share bands between fixed satellite services (FSS) and 5G NR, characterize the land mobile satellite channel at mm-waves, and study the applicability of 5G NR beam management for carrying out basic pointing procedures. The intention of this work is to contribute to the development of new space based NB-IoT networks so that the current terrestrial NB-IoT standard can be extended allowing an accessible data connection in un-served and under-served areas. Notice that NB-IoT technology has been considered as an integrated part of the first full set of 5G standards (i.e. 3GPP Release 15).

The standard for 5G Non-Terrestrial Networks (NTN) including NB-IoT NTN is planned for 3GPP Release 17 which is being developed in the coming months. Therefore, this work has been proposed to study different aspects regarding the implementation of a direct access between a NB-IoT device and a LEO satellite. Providing massive access while reducing the amount of collisions requires to point to the devices by employing narrow-beams, and this is possible at mm-waves. Recent physical layer structures for LEO satellite communications such as the one presented in [5], proposes a very interesting architecture for providing direct access between an UE and a LEO satellite.

However, this project is focused on the case where the UE is a NB-IoT device, and further characterization needs to be considered than in recent studies. In 3GPP [6], IoT devices have been only considered operating in S-Band, and this work addresses the link budget feasibility for the Ka-Band. In addition, this feasibility has been studied for the different type of NB-IoT transmissions, considering single-tone and multi-tone transmissions.

Regarding the proposed RSBA scheme, which has previously shown a good performance in terrestrial networks in terms of probability of collision and achievable rate [7] , further studies have to be carried out in order to implement it in a non-terrestrial scenario. Therefore, this project studies the practicability of a blind beamformer for massive access at Ka-Band in NR after concluding a multi-antenna channel between the NB-IoT devices and the LEO satellite and studying the feasibility of the link budget between the devices and the satellite.

It is important to highlight that the contribution of this work is focused on the uplink (UL), but could be extrapolated to the downlink (DL) too.

Summarizing, the contribution regarding 5G NR, is to deal with a NB-IoT scenario with massive devices in combination with beamforming techniques at the LEO satellite at Ka-Band in order to provide reliable communications by re-using frequency resources via NOMA access.

## 1.3 Thesis Organization

The remainder of the work is organized as follows. In Chapter 2, the LEO Sat-IoT system architecture is presented, including the hybrid multibeamforming implementation. Chapter 3 shows the main characteristics of LEO satellite communications at Ka-Band (e.g. different attenuations, satellite coverage, propagation delay, and Doppler shifts). In Chapter 4, technical challenges regarding 5G NR are presented. Chapter 5 deals with the beamforming technique implemented at the LEO satellite combined with the NOMA solution, including both mathematical developments and simulations. Finally, the last chapter presents the conclusions obtained and future work.

# Chapter 2

# Non-Terrestrial Network (NTN) System Architecture

## 2.1 LEO Sat-IoT System Architecture

The Non-Terrestrial Network (NTN) architecture presented in Fig.2.1 involves direct access between the satellite(s) and the on-ground NB-IoT devices by means of the NR air interface. This air interface, which is currently only specified for terrestrial systems, raises the importance of taking into account the typical LEO satellite channel impairments such as the large delays, the Doppler shifts due to the relative motion between the satellite and the user terminal, and the geographical area where the NB-IoT is located (e.g. sub-urban or rural). The impact of these channel impairments has to be assessed for both, the Physical Layer (PHY), and PHY/MAC procedures (e.g. Random Access, Timing Advance, and Hybrid-Automatic Repeated Request) [8].

There are two possible options of satellite payload implementations in the NTN architecture. On the one hand, a transparent or bent-pipe satellite, which basically receives the NB-IoT uplink signals, amplifies the received signals, transmits the signals to the NB-IoT devices, and if it is needed, it performs uplink-downlink frequency conversion. However, in this case, the 5G-RAN functionalities are not implemented at the satellite, and it just act as a flying relay node providing a "Satellite friendly" NR signal between the gNB and the NB-IoT devices in a transparent manner. On the other hand, the one which is implemented in the architecture presented below, is the regenerative transponder. With a regenerative satellite, it has the sufficient on board processing capabilities to be able to deploy gNB or Relay Node functions. Thus, it is capable to generate/receive a "Satellite friendly" NR signal to/from the NB-IoT devices.

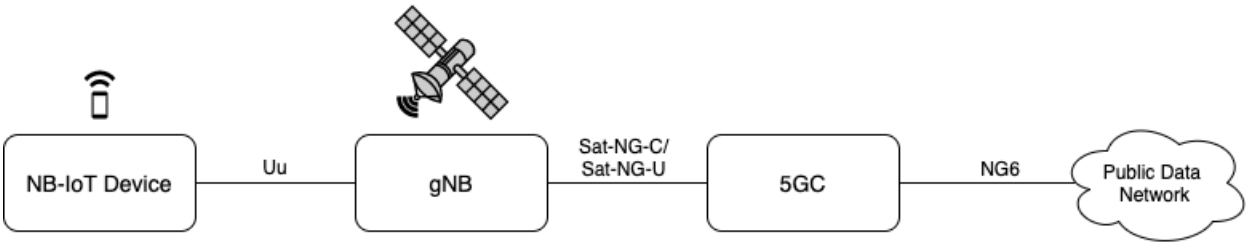


Figure 2.1: System Architecture based on a Satellite with gNB on board.

## 2.2 Hybrid Multibeamforming Satellite System

To attain a deeper insight on the system, a more detailed NTN is depicted in Fig.2.2, where the main components of a satellite communication system are shown [6].

- Satellite: a space-borne vehicle embarking a regenerative payload telecommunication transmitter, placed into Low-Earth Orbit (LEO) at 600 km altitude. It performs radio frequency filtering, frequency conversion and amplification, as well as demodulation/decoding, switch and/or routing, coding/modulation.
- NB-IoT device: terminal characterized by cost efficiency and low power consumption, which is connected directly to the satellite via NR air interface.
- Gateway: a ground station that interconnects the satellite to the 5G Core Network (5GC).
- Feeder Link: a radio link between the gateway and the satellite. This radio link can use any suitable air interface (e.g. existing SatCom standards such as DVB-RCS or DCB-S2X) or an adapted version of the NR air interface (i.e. NG-C/NG-U).
- Service Link: a radio link between the terminal and the satellite. In this architecture, the air interface is provided by the terrestrial NR. Thus, the impact of the different satellite channel impairments has to be assessed.

Since modern LEO satellites allows to employ both analog and digital beamforming, it is proposed to design a system that implements hybrid beamforming via large-scale phased array antenna system. This solution seems to adapt very well to the necessity of pointing specific areas by employing narrow-beams, and thus, increase the directivity of the antennas and compensate the higher propagation losses at satellite mm-wave communications [9] [10].

Conventional fully digital beamforming techniques are not feasible to implement at high frequencies with hundreds of antenna elements as it requires to implement one digital-to-analog (DAC) converter per antenna element. In other words, they demand a separate radio frequency (RF) chain for each antenna element. Even the flexibility and the high spectral efficiency that a fully digital

beamforming solution provides, it is costly and the power consumption is high at mm-wave systems with large-scale antenna arrays. Differently, analog beamforming is the most suitable solution for large-antenna systems at high frequencies. In this case, multi-antenna processing is applied after the digital-to-analog conversion, and only one DAC per layer is needed. However, this technique is very poor in flexibility and cannot fully exploit the available spatial resource.

As an alternative approach, hybrid beamforming is a promising solution in mm-wave systems, allowing to reduce costs supporting spatial multiplexing with a limited number of radio frequency (RF) chains. If it is compared with analog beamforming, hybrid beamforming supports multi-layer transmission with spatial multiplexing, as well as spatial division multiple access. In terms of spectral efficiency achieved, it is comparable to a fully digital beamforming solution with much reduced hardware complexity and costs. In particular, a qualitative comparison of different hybrid beamforming hardware implementations is performed in [10] where it shows that a group-connected mapping strategy with a fixed phase shifter (FPS) hardware implementation (i.e. $N$ fixed phase shifters shared by all RF chain-antenna pairs) stands out as a promising candidate to support hybrid beamforming in 5G and beyond mm-wave systems.

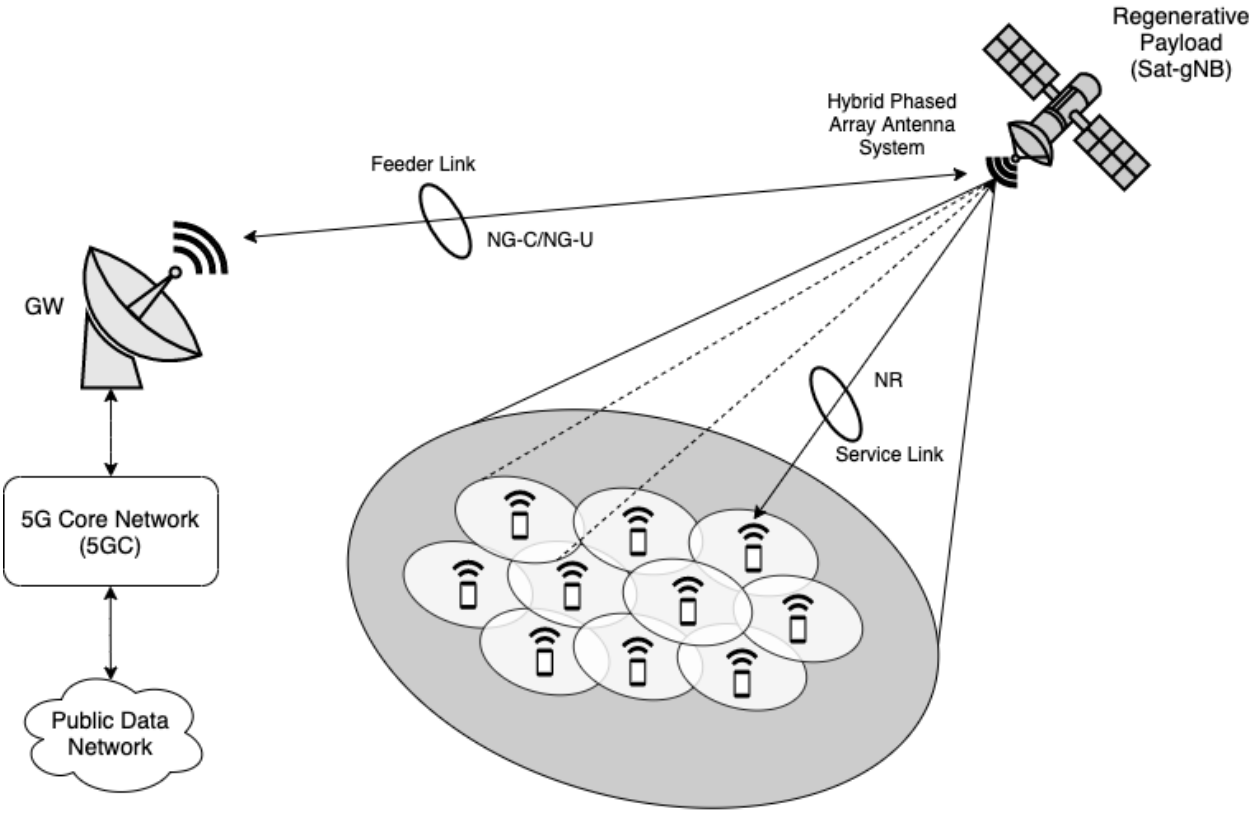


Figure 2.2: Multibeam Satellite System via Hybrid Beamforming for 5G NR Direct Access.

The architecture presented in Fig.2.2 follows a similar approach than the recently new physical layer structure for LEO satellite communication presented in [5], particularly in the hybrid multi-beamforming implementation. Nevertheless, along this work, a particular type of beamforming technique will be presented while maintaining the narrow-band condition, and thus satisfying a flat frequency response in the band of interest. According to ITU, many of mm-waves bands are shared with terrestrial services, and dedicated beamforming to the UEs will greatly reduce interferences and will provide better shared spectrum usage.

Despite parabolic antennas are more common in satellite communications scenarios, at Ka-Band, direct radiating active phased array antennas are capable of generating multiple simultaneous spot beams as it has been demonstrated in [11] and [12]. Besides, the architecture for the third generation relay satellites to be launched in the next decade or two at Ka-Band is currently being investigated by the National Aeronautics and Space Administration (NASA), and in fact, they have investigated the feasibility of designing a direct radiating phased array antenna for limited field-of-view [13]. It can be concluded that in the scenario considered in this work, flexibility is a must since the LEO satellite has to deal with massive access. For phased array antenna systems like the one proposed in this work, it is flexible to steer its radiation pattern to any designed angle with only change in phased shifting or amplitude. Meanwhile, if a parabolic antenna system is considered, it will be more difficult to steer the whole parabolic antenna. A detailed comparative study between parabolic and phased array antennas can be found in [14].

In the 5G context, such implementation in a LEO satellite poses severe challenges to the realization of a satellite-based 5G NR network. That requires, at first, to asses the impact of large delays and Doppler shifts due to the satellite movement, the channel propagation conditions, and the satellite elevation in the 5G NR system, particularly in a NarrowBand-IoT (NB-IoT) scenario.

# Chapter 3

# Characteristics of LEO Satellite Communications at Ka-Band

## 3.1 Channel Modeling

In the last decade, satellite communication systems have moved to frequency bands above 10 GHz to exploit the large bandwidth available and provide high data rates. However, at these frequency bands, the satellite link is degraded by different factors such as rain, cloud, and gaseous attenuation, as well as tropospheric scintillations [15].

- Attenuation due to precipitation: When propagating through snow, hail, ice droplets and, predominantly, rain, radiowaves suffer from hydrometeor scattering and absorption. Its effect can be predicted employing the empirical model proposed in ITU-R Recommendation P.618 [16].
- Cloud Attenuation: The liquid water content of clouds is the physical cause of cloud attenuation. Prediction models for this particular attenuation factor have been developed within the framework of ITU-R Recommendation P.840 [17].
- Gaseous Attenuation: The gaseous absorption, mostly from oxygen and water vapor, contributes to the total attenuation of radiowaves, especially in the case of low elevation angles. However, the contribution of gaseous absorption to the total attenuation is small compared to the attenuation due to rain. A complete method for calculating the gaseous attenuation is given in Annex 1 of ITU-R Recommendation P.676 [18].
- Tropospheric Scintillations: The variations in the magnitude and the profile of the refractive index of the troposphere lead to amplitude fluctuations known as scintillations. These fluctuations increase with the carrier frequency of the signal, being especially significant above

10 GHz. Besides, this effect increase with low elevation angles, due to the longer path of the signal, and wide beam width receiving antennas. An empirical model estimating the effect of scintillations on the received signal can be found in ITU-R Recommendation P.618 [16].

Furthermore, other relevant effects impairing satellite communications at Ka-Band are: the signal depolarization, the melting layer attenuation, and the sky noise increase. Given the difficulties due to the extend of interdependence between separate propagation effects, different modeling approaches have been considered. For example, a first approach considers all attenuation effects as being correlated, while another approach treats attenuation effects as being partially uncorrelated; therefore, Root Mean Square (RMS) is adopted for the total attenuation. A combination method that considers the some of the effects as being uncorrelated is proposed in [16], which it will be used in this work. The total atmospheric attenuation over the satellite link is given by:

$$A_{tot} = A_{O_2} + A_{H_2O} + \sqrt{(A_C + A_R)^2 + A_S^2} \tag{3.1}$$

where $A_{O_2}$,$A_{H_2O}$,$A_C$,$A_S$, stand for the attenuation due to oxygen, water vapor, cloud, rain, and scintillation, respectively.

Based on this, LEO satellite communication links with UEs at low elevation angles (i.e. $\theta_{UE} \leq 20°$) for long periods of time will be highly affected by the atmosphere. In [4], the total atmospheric attenuation versus elevation angle for a hypothetical link in Berlin employing the prediction models in [16] is shown. Given this, for a frequency of 20 GHz it can be stated that the total atmospheric attenuation is lower than 5 dB for $\theta_{UE} \geq 40°$. However, it is expected that a constellation of LEO satellites will provide direct access to the UEs at relatively high elevation angle.

Aside from the atmosphere attenuation, the understanding of how the shadowing and multipath behaves in various environments (e.g. urban, suburban, and tree shadowed) and the satellite elevation angles are becoming important aspects of study [4].

The proposed architecture employs highly directional beams pointing to the NB-IoT devices, assuming that line-of-sight (LOS) or nearly-LOS channel conditions exists (i.e. the UE needs to be outdoors in order to receive from a satellite). When a fading process has a LOS component $A_c$ together with multipath fading, the channel is modeled as Rician [19]. The Rice process is given by:

$$a_r(t) = \mathrm{Re}\{[A_c + a_c(t) + ja_s(t)]\exp[j2\pi f_c t]\} \tag{3.2}$$

and its envelope $r$ and phase $\phi$ are given by

$$r = \sqrt{[A_c + a_c(t)]^2 + a_s^2(t)} \tag{3.3}$$

$$\phi = \tan^{-1}\left(\frac{a_s}{A_c + a_c}\right) \tag{3.4}$$

where

$$a_c(t) = \mathrm{Re} \sum_{k=-N/2}^{N/2} V_k \exp[j(2\pi k f_0 + \lambda_k)] \tag{3.5}$$

$$a_s(t) = \mathrm{Im} \sum_{k=-N/2}^{N/2} V_k \exp[j(2\pi k f_0 + \lambda_k)] \tag{3.6}$$

$V_k$ is the amplitude and $\lambda_k$ is a random phase angle uniformly distributed between 0 and $2\pi$. N is the number of sinusoids, $Re$ denotes the "real part of", and $Im$ denotes the "imaginary part of".

As it is expected, in the case of dense urban scenarios and low elevation angles, the LOS component is blocked. This might not be an issue since the main target of the satellite communication systems is to complement and extent terrestrial networks, especially for sub-urban and rural scenarios. In fact, if shadowing is considered, the Land Mobile Satellite Fading Channel described in [19], which assumes that the LOS component under shadowing conditions is log-normally distributed and the multipath effect is Rayleigh distributed, could be a channel model candidate for NTN under shadowing conditions. However, further experimental channel campaigns are needed to determine the model for NTN under different scenarios and elevation angles. The European Space Agency (ESA) has already issued an ITT under the ARTES AT programme with the objective of characterizing the land mobile satellite channel in terms of shadowing, clutter and multipath low gain UEs at mm-waves.

In the next chapter, more information about the link budget and the delay spread in satellite propagation channels will be shown.

## 3.2 LEO Satellite Coverage

The scope of this section is to study the time window where a LEO satellite is visible over a certain angle of elevation with respect to the UE. Considering the wide services capabilities, the unlimited coverage provided by satellite constellations, and the reduced vulnerability of satellites to physical attacks and natural disasters, makes satellite communication systems a promising solution to extend and complement terrestrial networks. Particularly, providing 5G services in un-served and under-served areas that cannot be covered by terrestrial networks.

Typically, a satellite into Low-Earth Orbit (LEO) is placed at an altitude between 500 km to 2000 km, and due to the movement of the satellite, is visible to a ground UE for a few minutes or even for seconds at high elevation angles. In Fig.3.1, it is depicted how LEO satellite communications with polar orbiting satellites vary the coverage in time, in particular at an height of 600 km.

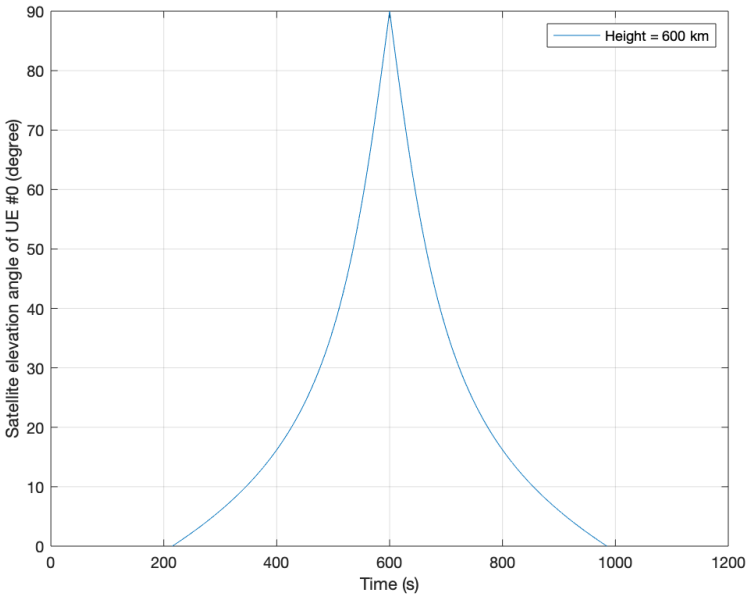


Figure 3.1: Elevation of the LEO Satellite (h=600 km) as a function of time with respect to the on-ground fixed NB-IoT device.

In addition, Table 3.1, summarizes the time window where a LEO satellite is visible over specific angles of elevation with respect to the fixed on-ground UE. The typical minimum elevation angle for terminals in NGSO satellite based systems is in the range of $\theta_{UE} = 10°$ to $\theta_{UE} = 30°$, while ensuring service continuity optimizing the number of satellites [6].

A very recent study [4] states that, due to the sharp increase of tropospheric and other attenuation factors at low elevation angles in mm-waves NGSO satellite communications, a minimum elevation angle of $\theta_{UE} = 40°$ is assumed, specifically having a single satellite visible at elevation higher than 40° globally. It is worth mentioning that this approach consider that the NGSO satellite always transmits in the downlink at the maximum power allowed while assuring the protection of the terrestrial services. This protection comes in the form of a Power Flux Density (PFD) over a reference bandwidth [dbW/$m^2$ over 1 MHz], which depends on the elevation angle. Concluding this section, if it is assumed that the minimum elevation is $\theta_{UE} = 40°$, a single LEO satellite orbiting at an height of 600 km will be visible over the minimum elevation angle approximately during 3 minutes.

| **LEO $h_{sat}$ = 600 km** | |
|---|---|
| **Elevation angle $\theta$** | **Time window [s]** |
| $\theta_{UE} > 5°$ | 624.9 |
| $\theta_{UE} > 10°$ | 509.2 |
| $\theta_{UE} > 20°$ | 347.8 |
| $\theta_{UE} > 30°$ | 246.8 |
| $\theta_{UE} > 40°$ | 179 |
| $\theta_{UE} > 50°$ | 129.4 |
| $\theta_{UE} > 60°$ | 90.4 |
| $\theta_{UE} > 70°$ | 56.7 |
| $\theta_{UE} > 80°$ | 28 |

Table 3.1: Time window duration in function of the elevation angle with respect to the fixed on-ground UE.

### 3.2.1 Beam Pointing

As it is mentioned before, in mm-waves and employing large-scale antenna arrays, hybrid-beamforming techniques allows to create highly directional beams between the satellite (i.e. flying gNB) and the UEs. This fact is inline with beam-centric paradigm of 5G NR in the FR2, which includes the frequencies in the range between 24.25 GHz and 52.6 GHz. In the presented scenario, the LEO satellite generates several beams over a given area, which in the end, they will point to the device of interests (e.g. through digital beams inside the analog beam) with the objective of increasing the Signal-to-Noise Ratio (SNR). Typically, the footprint of the beams are elliptic shape and the radius of spots beams depend on the satellite communications system design, which it can range from tens of kilometers to a few thousands of kilometers. According to the example provided in [5], with a satellite phased array antennas structure of 21x21x4x4 antenna elements, the pointing beam width is 0.38°, which is traduced in a 4.6 km spot beam on earth surface.

It is important to consider that, for a non-geostationary satellite, the footprint may sweep over the earth's surface with the satellite movement (i.e. satellite fixed coverage) or may be earth fixed. To deploy a satellite constellation that provides earth fixed coverage (EFC), beam pointing mechanism are needed to compensate the movement of the satellites. But also a good synchronization is needed to avoid loss of sequence or even loss or duplication of coverage. In addition, the propagation delay differences between the different satellites in view should be compensated. Figure 3.2, depicts the distance between UE and the center of spot beam as a function of time. Note that the UE will be located at the center of the footprint at $\theta_{UE} = 90°$.

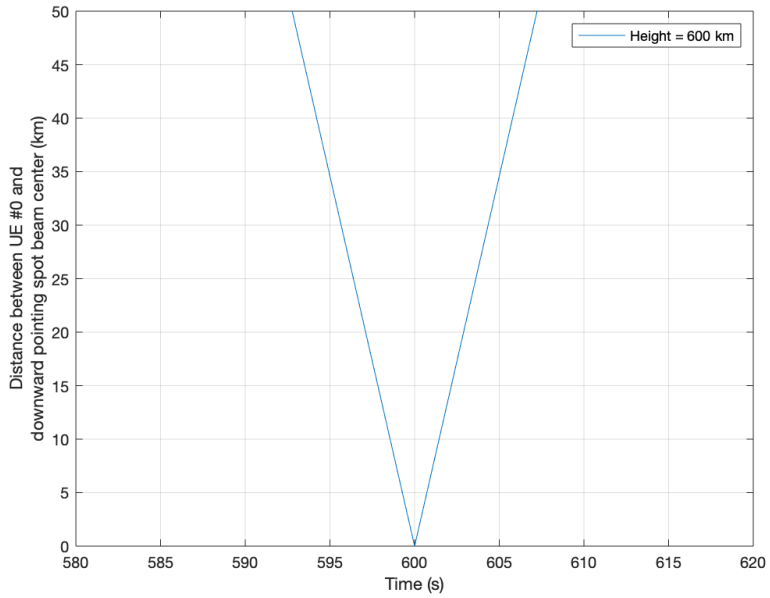


Figure 3.2: Distance between UE and the center of downward pointing spot beam as a function of time.

According to the figure presented before, it shows that, if the footprint radius is 35 km, the spot beam from a NGSO satellite at the height of 600 km will cover the UE for approximately 10 seconds. That means for the case of narrower beams, the satellite will cover the UE for a very few seconds. In these conditions, multi-beam satellites with satellite fixed coverage (SFC) employing narrow beams, will result in frequent hand-offs causing inefficient channel resource utilization, high processing costs and overall, lower system capacity.

One might think that another alternative to avoid the use of adaptive beamforming mechanism while reducing the handoff overhead is the use of some specific terrestrial 5G NR features. Nevertheless, NR beam management for mobility between spot-beams on the same gNB cannot be used by satellite systems to minimize the handoff overhead. Basically, this procedure might assume same frequency on the adjacent beams, but in the case of a multibeam satellite communication, these beams may use different frequencies or different polarization. Consequently, there is a need to adapt the beam management procedure for satellite communication systems, especially for NGSO.

## 3.3 LEO Satellite Propagation Delay

Regarding terrestrial 5G networks, where the Round Trip Time (RTT) between the base station and the UE is usually within 1 ms, the propagation delay in LEO satellite systems, depending on the system architecture (i.e. transparent payload or flying-gNB) it might be an issue or in

the best case (e.g. at high elevation angles), it can be four or five times the propagation delay observed in terrestrial networks. As the architecture presented in Fig.2.2 employs a regenerative payload, which is more complex and costly than a transparent payload implementation, allows to reduce significantly the propagation delay. Moreover, if any modifications are needed in the PHY, MAC or upper layers, it can be done directly in the flying-gNB without requiring to perform this modification in the gateway as it will be done in a transparent payload implementation system architecture.

Considering the system architecture presented in this work, the RTT can be calculated as approximately twice the propagation delay between the satellite and the UE, considering the on-board signal processing time negligible with respect to the propagation delay. Thus, assuming that the radio signal propagates at the speed of light in vacuum, the RTT can be computed as follows:

$$RTT \approx 2T_{gNB-UE} = 2\frac{d_{gNB-UE}(\theta_{UE}(t))}{c} \tag{3.7}$$

The LEO satellite elevation angle varies with the time, as the distance between the transmitter and the receiver does. Figure 3.3, depicts the distance between the UE and the satellite as a function of the elevation angle. Note that if the UE is underneath the LEO satellite (i.e. $\theta_{UE}$=90°), the distance between corresponds to the 600 km LEO satellite height.

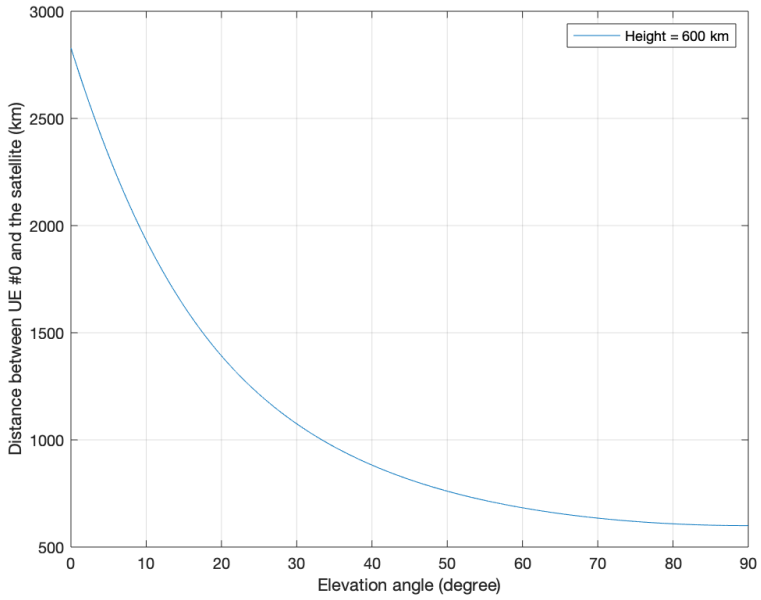


Figure 3.3: Distance between UE and the satellite as a function of the elevation angle.

In addition, Figure 3.4 and Figure 3.5 depicts the one-way propagation delay between the satellite and the UE in function of time, and in function of the satellite elevation angle, respectively.

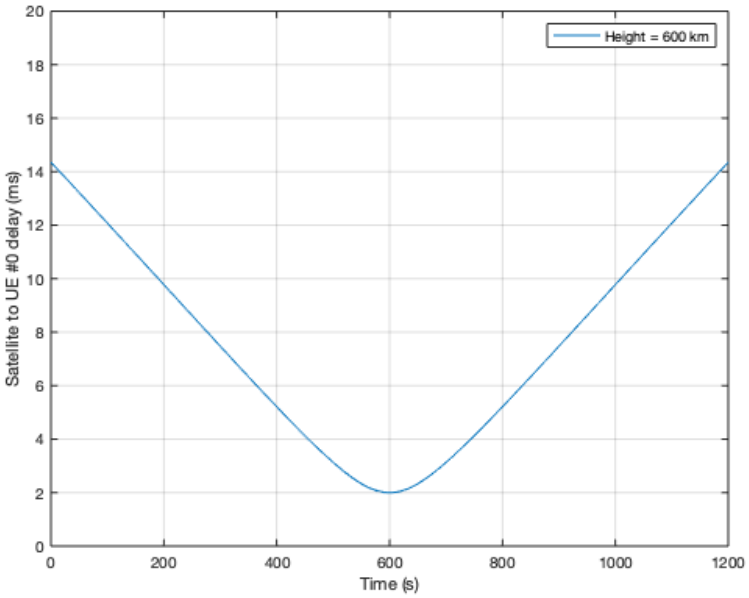


Figure 3.4: One-way propagation delay between UE and the satellite as a function of time.

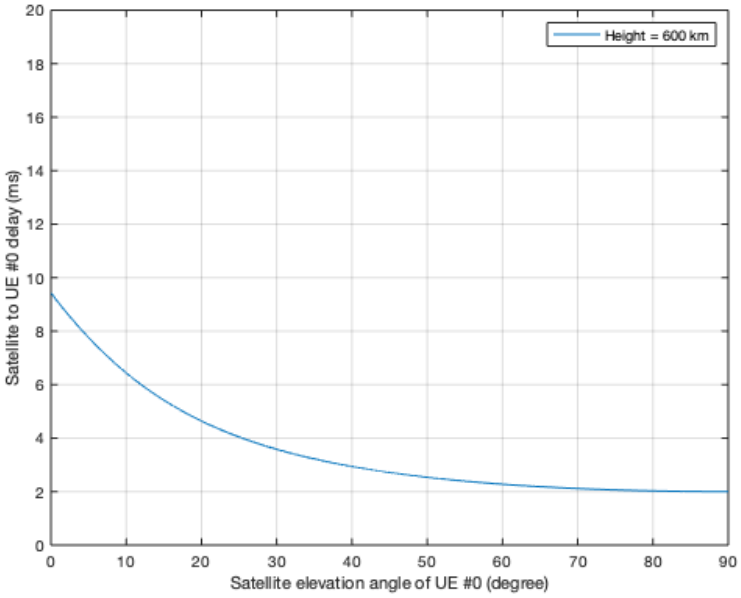


Figure 3.5: One-way propagation delay between UE and the satellite as a function of the elevation angle.

To summarize this section, the single path distances between the UE and the LEO satellite, the related propagation delays, and the approximated RTTs are listed in Table 3.2.

| **LEO $h_{sat}$ = 600 km** | | | |
|---|---|---|---|
| **Elevation angle $\theta$** | **Distance [km]** | **One-way [ms]** | **RTT [ms]** |
| $\theta_{UE} = 5°$ | 2329 | $\approx 7.76$ | $\approx 15.52$ |
| $\theta_{UE} = 10°$ | 1932 | $\approx 6.44$ | $\approx 12.88$ |
| $\theta_{UE} = 20°$ | 1392 | $\approx 4.64$ | $\approx 9.28$ |
| $\theta_{UE} = 30°$ | 1075 | $\approx 3.58$ | $\approx 7.16$ |
| $\theta_{UE} = 40°$ | 882.4 | $\approx 2.94$ | $\approx 5.88$ |
| $\theta_{UE} = 50°$ | 760.8 | $\approx 2.54$ | $\approx 5.08$ |
| $\theta_{UE} = 60°$ | 683.1 | $\approx 2.28$ | $\approx 4.56$ |
| $\theta_{UE} = 70°$ | 634.9 | $\approx 2.12$ | $\approx 4.24$ |
| $\theta_{UE} = 80°$ | 608.5 | $\approx 2.03$ | $\approx 4.06$ |
| $\theta_{UE} = 90°$ | 600 | $\approx 2$ | $\approx 4$ |

Table 3.2: Time window duration in function of the elevation angle with respect to the on-ground UE.

## 3.4 LEO Satellite Doppler Shift

The Doppler shift can be described as the change in the carrier frequency due to the movements of the transmitter, receiver, and/or objects in the scenario. However, in the aforementioned scenario, the Doppler shift will be clearly significant due to the movement of the satellite, which is approximately 7.56 km/s at 600 km of height. It is important to highlight that in the case of terrestrial networks, 5G NR can maintain a sufficient Quality of Service (QoS) even at a maximum UE speed of 500 km/h (e.g high speed train). For example, a typical terrestrial network operating at 2 GHz has a Doppler shift of less than 1 kHz even for high speed UEs, which can be easily handled by 5G NR.

In order to asses the impact of Doppler shifts on the 5G NR specifications, a closed-form expression of the Doppler shift as a function of the elevation angle and the satellite angular velocity (with respect to the UE) will be computed [20]:

$$f_d(t) = \frac{f_c \cdot \omega_{sat-gNB} \cdot R_E \cdot \cos(\theta_{UE}(t))}{c} \tag{3.8}$$

where $\omega_{sat-gNB} = \sqrt{GM_E/(R_E + h_{sat})^3}$ the angular velocity, $R_E = 6371$ km the Earth radius, $G = 6.67 \cdot 10^{-11}\text{Nm}^2/\text{kg}^2$ the Gravitational constant, and $M_E = 5.98 \cdot 10^{24}$ kg the Earth mass.

Figure 3.6, shows how the absolute value of Doppler shift changes in function of the elevation angle, detailed values can be found in Table 3.3. To cope with the considerable difference between the terrestrial and non-terrestrial Doppler shifts, the compensation of the effects of the large Doppler shifts caused by LEO satellite movement is needed. This Doppler compensation can be performed at the UEs or the satellite. Both options might rely on GNSS systems, which provides useful information (e.g. actual position of the satellite and the UE) and it seems to be a suitable solution [20].

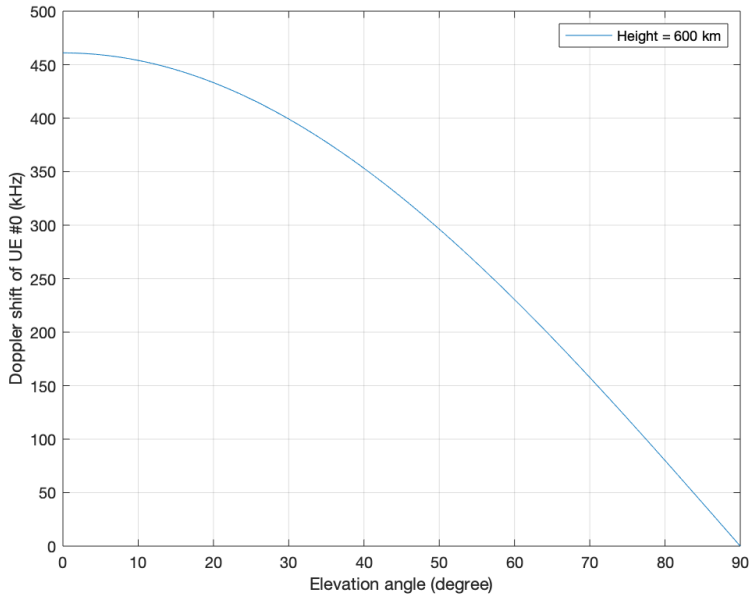


Figure 3.6: Absolute value of Doppler shift in function of the elevation angle between the UE and the LEO satellite with $f_c$=20 GHz.

| **LEO $h_{sat}$ = 600 km** | |
|---|---|
| **Elevation angle $\theta$** | **Doppler shift [kHz]** |
| $\theta_{UE} = 5°$ | 459.3 |
| $\theta_{UE} = 10°$ | 454 |
| $\theta_{UE} = 20°$ | 433.2 |
| $\theta_{UE} = 30°$ | 399.3 |
| $\theta_{UE} = 40°$ | 353.2 |
| $\theta_{UE} = 50°$ | 296.3 |
| $\theta_{UE} = 60°$ | 230.5 |
| $\theta_{UE} = 70°$ | 157.7 |
| $\theta_{UE} = 80°$ | 80 |
| $\theta_{UE} = 90°$ | 0 |

Table 3.3: Absolute Doppler shifts values in function of the elevation angles with $f_c$=20 GHz.

It is expected that satellite based 5G NR networks will handle mobility speeds up to 1000 km/h (e.g. aircrafts systems). Thus, NR features may require adaptations to support NR service via satellite. For example, the sub-carrier spacing (SCS) of 5G NR signals may be extended with greater SCS values to compensate large Doppler shifts.

# Chapter 4

# Direct Access to 5G NR Technical Challenges

## 4.1 Physical Layer

Orthogonal Frequency Division Multiple Access (OFDMA) technique is used in 5G NR as the baseline for both downlink and uplink transmissions. In addition, it is possible to use DFT-precoded OFDMA (i.e. SC-FDMA) in the uplink. Different from LTE where SC-FDMA in the UL is a must, in 5G NR is optional. The main reasons for considering OFDMA in the UL are: spatial multiplexing receivers become more complex with SC-FDMA, it is beneficial to maintain symmetry between UL and DL transmission schemes, and SC-FDMA imposes scheduling restrictions (e.g. contiguous allocations in the frequency domain) while OFDMA allows a more flexible allocation. However, Single Carrier Frequency Division Multiple Access (SC-FDMA) reduces the peak-to-average power ratio (PAPR) and consequently the expensiveness of the UEs. For this reason, SC-FDMA has been selected as the technology for the UL in NB-IoT technology, and thus for the satellite-based 5G NR network presented in this work.

In 5G NR, OFDMA supports different subcarrier separation $\Delta f$, denoted as numerologies:

| **Subcarrrier spacing** $\Delta f$ [kHz] | **Symbol duration** $T_u = 1/\Delta f$ [$\mu s$] | **normal CP length** [$\mu s$] | **extended CP length** [$\mu s$] | **Frequency range** |
|---|---|---|---|---|
| 15 | 66.67 | 4.69 | Not defined | FR1 |
| 30 | 33.33 | 2.34 | Not defined | FR1 |
| 60 | 16.67 | 1.17 | 4.16 | FR1/FR2 |
| 120 | 8.33 | 0.59 | Not defined | FR2 |
| 240 | 4.17 | 0.29 | Not defined | FR2 |

Table 4.1: 5G NR numerologies.

Regarding Table 4.1, it is important to remark that the cyclic prefix of the 1st symbol every 0.5

is 0.52 $\mu$s longer than the value in the table. At frequencies below 6 GHz (i.e. FR1 frequency range), low values of $\Delta f$ are better because they allow having longer cyclic prefix duration, needed to counteract the longer delay spread associated to large cells. On the other hand, at mm-waves (i.e FR2 frequency range), high values of $\Delta f$ are useful to counteract frequency errors and phase noise. In this case, the cyclic prefix can be shorted because cells are smaller and beamforming is extensively used, so delay spread is also smaller. However, these configurations have been set for terrestrial 5G NR networks. Then, the NTN channel model delay spread should be studied in order to assess the compatibility with the existing cyclic prefix values.

## 4.2 Delay Spread in Satellite Propagation Channels

The delay spread measures the time difference between the time of arrival of the direct ray (i.e. LOS component) and the time of arrival of the last multipath components. ITU-R defines for the 2 GHz bad tree different models (i.e. A,B,and C), applicable for an elevation range from $\theta_{UE} = 15°$ to $\theta_{UE} = 55°$ and for urban, suburban and rural environments. Note that the most restrictive channel is C (see Fig.4.2), whereas the 250 ns are stated to cover 90% of the cases.

| **Tap number** | **Relative tap delay value (ns)** | **Tap amplitude distribution** | **Relative Power (dB)** |
|---|---|---|---|
| 1 | 0 | LOS: Rice<br>NLOS: Rayleigh | 0.0<br>-12.1 |
| 2 | 60 | Rayleigh | -17.0 |
| 3 | 100 | Rayleigh | -18.3 |
| 4 | 130 | Rayleigh | -19.1 |
| 5 | 250 | Rayleigh | -22.1 |

Table 4.2: ITU-R M.1225 Channel Model C.

In case of a satellite communication channel with LOS or nearly-LOS conditions it is expected that for higher elevation angles (i.e. $\theta_{UE} \geq 55°$), the delay spread of the LEO satellite channel will be in the same range or even lower due to the traveling distances of the multipath components. Given the results for the delay spread measurements at Ka-Band in [21], the calculated maximum delay spread for omnidirectional antennas at 40 Ghz is $T_m = 25$ ns. Then, it can be assumed that for the case of directional antennas, or by using beamforming, the maximum delay spread will be even lower.

Focusing on Table 4.1, it is observed that lower numerologies (e.g. 15 kHz, 30 kHz) have an over-dimensioned CP, which provoke a slightly reduction of the spectral efficiency. In contrast, higher numerologies (e.g. 120 kHz or 240 kHz) CP lengths match well with the propagation characteristics in Ka-Band. Then, it can be stated that existing 5G NR cyclic prefix values adapts to the LEO satellite channel model delay spread.

## 4.3 Link Budget Analysis

In order to assess the feasibility of a direct link access between a NB-IoT device and a LEO satellite at Ka-Band, the link budget analysis will be performed. The general formula of the link budget, taking into account all the signal gains and losses in the propagation medium from transmitter to receiver, and considering that there are no interferences in the scenario, is given as follows [22]:

$$\begin{aligned} SNR(dB) = EIRP(dBW) + \frac{G_R}{T}(dBi/K) - FSPL(dB) - A_{loss}(dB) - Ad_{loss}(dB) \\ -K\left(\frac{dBW/K}{Hz}\right) - 10 \cdot log_{10}(BW) \end{aligned} \tag{4.1}$$

where

- $EIRP$ is the effective isotropic radiated power of the transmitting antenna and can be calculated as follows:

$$EIRP = 10 \cdot log_{10}(G_T P_T) \tag{4.2}$$

  where $G_T$ is the antenna gain and $P_T$ is the transmitting antenna power.

- $G_R/T$ is the figure of merit at the receiver with antenna gain $G_R$ and equivalent system temperature $T$ defined as follows:

$$\frac{G_R}{T} = G_R(dBi) - NF(dB) - 10 \cdot log_{10}\left(T_o + (T_a - T_o) \cdot 10^{-0.1 \cdot NF}\right) \tag{4.3}$$

  where $G_R$ is the receiving antenna gain, $NF$ represents the noise figure, $T_o$ is the ambient temperature, and $T_a$ is the antenna temperature.

- FSPL is the free space path loss given by:

$$FSPL = 10 \cdot log_{10}\left(\frac{4\pi D}{c/f_c}\right)^2 \tag{4.4}$$

  where $f_c$ is the carrier frequency, $c$ the speed of light, and $D$ the distance between the UE and the satellite, also known as slant range. Note that this distance varies with the time as the elevation angle is changing. More detailed values about the slant range can be found in Table 3.2.

  The FSPL of the scenario described in this work, represented as a function of the elevation angle, can be found in Figure 4.1. It is important to notice that the free space path losses depend also in the height of the satellite. Considering that the UE is underneath the LEO satellite (i.e. $\theta_{UE} = 90°$) the slant range corresponds to the LEO satellite height.

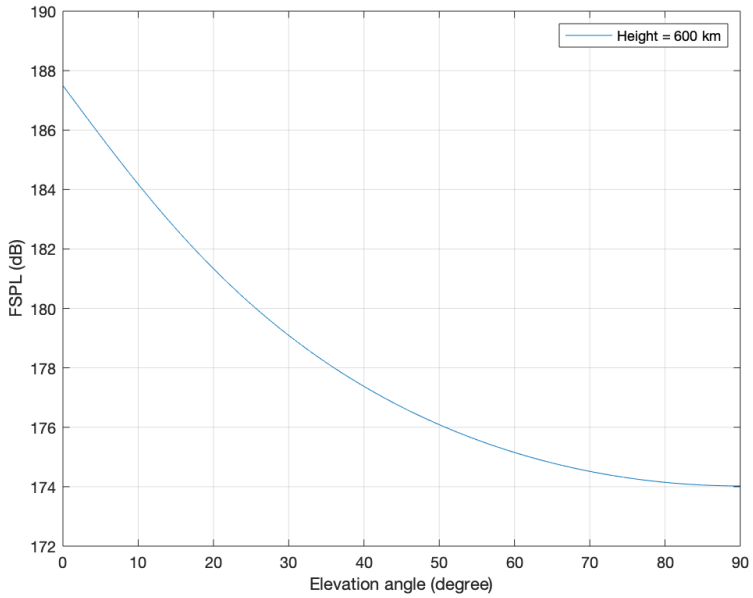


Figure 4.1: Free space path loss as a function of the elevation angle $\theta_{UE}$ at $f_c$=20 GHz.

- $A_{loss}$ represents the atmospheric looses and $Ad_{loss}$ the additional looses due to the feeder link.
- $K$ is the Boltzmann constant and $BW$ is the communication bandwidth.

At starting point, the following assumptions has been considered for the uplink budget: an UE EIRP of 23 dBm and a LEO satellite at 600 km with $G_R/T$ = 13.5 dB/K. The UE parameters are defined in the NB-IoT standard for 3GPP Class 3 devices, which can be found in [6], are summarized in Table 4.3.

| | **IoT device (3GPP Class 3)** |
|---|---|
| **Transmit Power** | 200 mW (23 dBm) |
| **Antenna Type** | Omnidirectional antenna (linear polarisation) |
| **Antenna Gain** | Tx and Rx: 0 dBi |
| **Noise Figure** | 9 dB |
| **EIRP** | -7 dBW |
| **G/T** | -33.6 dB/K |
| **Polarisation** | Linear |

Table 4.3: IoT device (Class 3) 3GPP defined parameters.

It is important to highlight that some parameters are fixed or determined a-priori, due to regulatory aspects, like the peak EIRP upper limit specified by the Federal Communications Commission (FCC), or due to the terminal form factor.

5G NR allows channel bandwidths up to 400 MHz without employing carrier aggregation. However, there are many UEs that cannot support this maximum bandwidth due to device capabilities (e.g. IoT device) or energy consumption. Figure 4.2 represents the uplink SNR at 20 GHz for different elevation angles using a channelization of 100 MHz. In this case, any fading has been considered, and the atmospheric losses are the ones obtained for 20 GHz in [4]. Along with the 23 dBm peak EIRP, also the upper FCC limit of 43 dBm has been considered.

In addition, it is important to underline that as starting point NB-IoT device limitations in terms of channel bandwidth have not been considered, as the main point is to observe the feasibility of a UE with an EIRP of 23 dBm with the proposed $G_R/T$. Further discussions related to NB-IoT device channel bandwidth will be presented during this section.

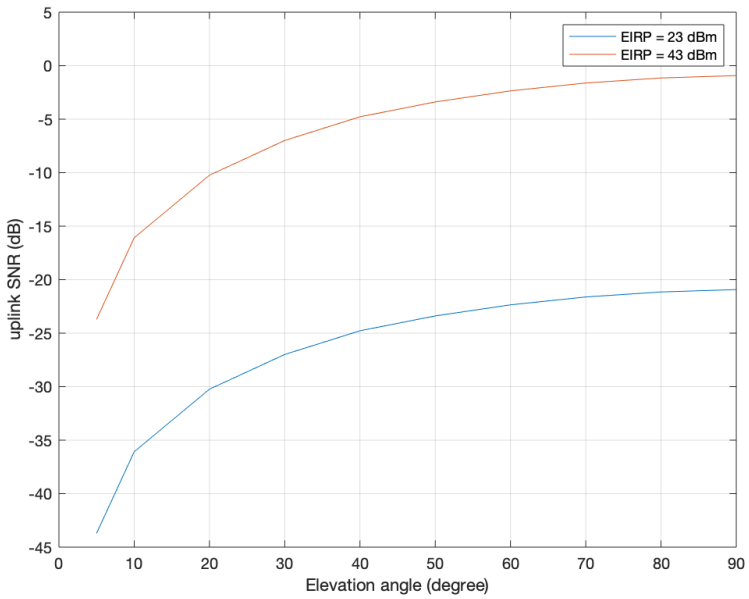


Figure 4.2: Uplink SNR versus elevation angle $\theta_{UE}$ at $f_c$=20 GHz with $G_R/T$=13.5 dB/K and BW=100 MHz.

It can be observed that a channelization of 100 MHz cannot be supported by a direct link between an UE and a LEO satellite at 600 km with the aforementioned conditions. In order to asses how the channel bandwidth impacts the uplink budget, Fig.4.3 depicts the uplink SNR for different channel bandwidths when the UE is underneath the LEO satellite (i.e. best conditions, $\theta_{UE} = 90°$).

Due to the difficulties of establishing the uplink communication, it is necessary to consider the minimum channel bandwidth allowed by 5G NR in FR2 while ensuring a relatively high elevation angle. Taking advantage of 5G NR features, such as the use of BandWidth Parts (BWP), it will allow certain UEs to operate only on a portion of the channel and will avoid the decodification of signals over the whole bandwidth. One BWP is defined as the minimum allowed 5G NR channel

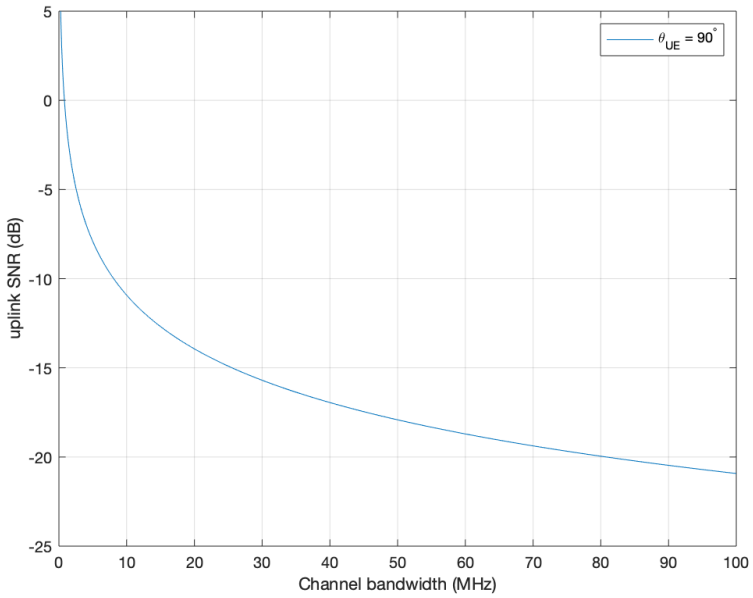


Figure 4.3: Uplink SNR versus the channel bandwidth at $f_c$=20 GHz with $G_R/T$=13.5 dB/K.

bandwidth, which is at least one Resource Block (RB) (i.e. 12 consecutive subcarriers in the frequency domain). Then, taking into account the different SCS (see Fig.4.1) in FR2, a SCS of 60 kHz will provide the minimum bandwidth, which is 720 kHz. Figure 4.4 represents the uplink SNR as a function of the elevation angle with 1 MHz channel bandwidth, rounding the aforementioned 720 kHz.

To attain a deeper insight on the scenario described in this work, the next simulations will be devoted to asses the feasibility of a reliable direct link between a NB-IoT device and a LEO satellite. The main advantage of NB-IoT is that it can be deployed within a 5G NR carrier by allocating one RB of 180 kHz (i.e. SCS of 15 kHz) to NB-IoT. Based on where the NB-IoT carrier is placed, it is considered three deployments options: standalone, guard-band, and in-band. Regarding the main features, NB-IoT downlink transmission uses OFDMA with SCS of 15 kHz, whereas the uplink transmission uses SC-FDMA with SCS of 3.75 kHz or SCS of 15 kHz. It is important to underline that the uplink supports two type of transmissions, single-tone (ST) and multi-tone (MT) transmissions (i.e. 3, 6, and 12 subcarriers). The ST option is more adequate for scenarios with poor coverage but the peak rate will be reduced if it is compared with the one achieved in MT transmissions.

Despite it was assumed an initial $G_R/T$ in the uplink, the EIRP and the $G/T$ of the LEO satellite should be carefully designed before launching new satellites to support NB-IoT services. The link reliability in NB-IoT systems is evaluated though the block error rate (BLER) associated with the specific MCS. As SNR is increased, BLER is decreased. 3GPP 4G LTE and 5G NR-standards are specified to set the target BLER of 0.1 (i.e. 10%). It is true that by using the HARQ operation the

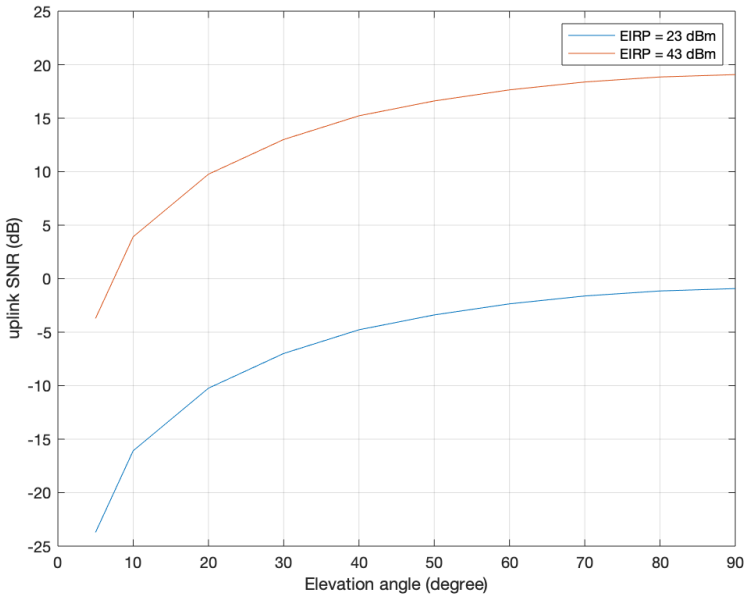


Figure 4.4: Uplink SNR versus elevation angle $\theta_{UE}$ at $f_c$=20 GHz with $G_R/T$=13.5 dB/K and $BW$=1 MHz.

link reliability would be improved, but for NR NTN satellite transmission, the number of HARQ processes may need to be further extended flexibly according to the induced RTT delay [6]. Given the required SNR values corresponding to a 10% BLER at the first HARQ transmission [23], an analysis is performed in order to obtain the spectral efficiency as a function of the satellite $G/T$ for the uplink transmission. The link budget parameters are summarized in Table 4.4.

| **Link Parameters** | **Uplink** |
|---|---|
| **Carrier Frequency [GHz]** | 20 |
| **Wavelenght [m]** | 0.015 |
| **Minimum Elevation Angle [degree]** | 40 |
| **Bandwidth [kHz]** | 3.75, 15, 45, 90, 180 |
| **Subcarrier Spacing [kHz]** | 3.75, 15 |
| **Satellite Altitude [km]** | 600 |
| **max EIRP per Carrier [dBm]** | 23 |
| **Link Distance [km]** | 882.4 |
| **FSPL [dB]** | 177.38 |
| **Atmospheric Losses @ 99%/95% [dB]** | 5 |
| **Additional Losses [dB]** | 1 |
| **Shadow Fading Margin (for std=4dB) @ 95% [dB]** | 0 |

Table 4.4: Uplink budget parameters.

Note that in the uplink analysis (see Fig.4.5), both type of transmissions ST and MT have been considered. For the MT case employing 12 subcarriers (i.e. 180 kHz of channel bandwidth) a minimum $G/T$ of 21 dB/K for a LEO satellite is needed. It can be observed that it is possible to close the link while achieving the peak spectral efficiency at lower $G/T$ values using other transmission modes (e.g. 1, 3 or 6 subcarriers). However, even though the peak spectral efficiency is reached by means of different transmission modes, this will have an impact on the overall system design. Choosing one transmission mode or another it will impact the whole NB-IoT system, including important aspects such as delay, capacity, and energy consumption. Further details regarding these aspects are discussed in [23].

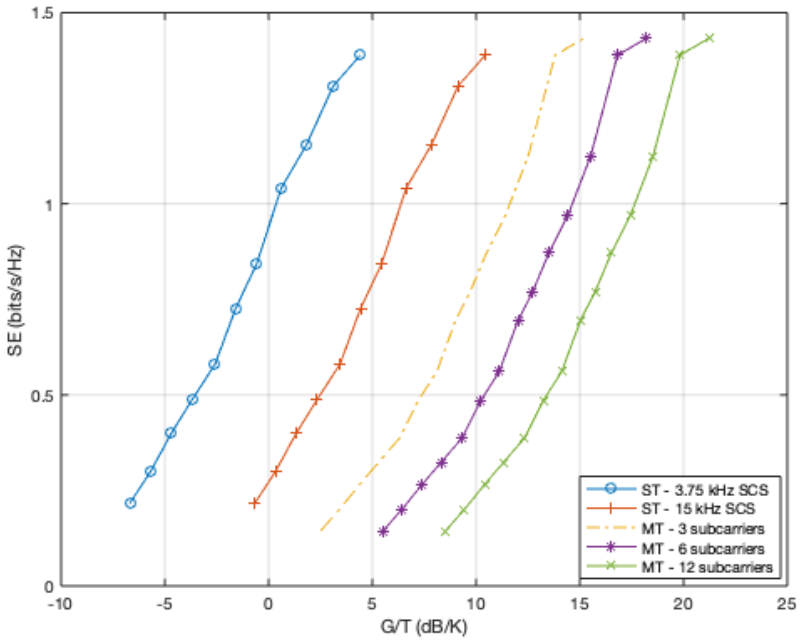


Figure 4.5: Link budget result for uplink transmission between a NB-IoT device and a LEO satellite.

Even thought the downlink is not a relevant aspect in this work, some insights are given. In the case of the downlink it is interesting to obtain the spectral efficiency as a function of satellite EIRP. As mentioned before, the satellite EIRP has to be carefully designed because this parameter would directly affect the received SNR. In addition, in order to protect the terrestrial services, a downlink power control that adapts to the max PFD limit will be needed. However, one of the main advantages of the Ka-Band (i.e. 20 GHz) is that there is no shared allocation with 5G FR2. Also, it is important to underline that there exists an exclusive satellite band of 500 MHz between 19.7 GHz and 20.2 GHz, meaning that it is only allocated to satellite services (FSS) and not to terrestrial services. The link budget parameters for the downlink analysis are summarized in Table 4.5 and the results are depicted in Figure 4.6.

| **Link Parameters** | **Downlink** |
|---|---|
| **Carrier Frequency [GHz]** | 20 |
| **Wavelenght [m]** | 0.015 |
| **Minimum Elevation Angle [degree]** | 40 |
| **Bandwidth [kHz]** | 180 |
| **Subcarrier Spacing [kHz]** | 15 |
| **Satellite Altitude [km]** | 600 |
| **NB-IoT device G/T [dB/K]** | -33.6 |
| **Link Distance [km]** | 882.4 |
| **FSPL [dB]** | 177.38 |
| **Atmospheric Losses @ 99%/95% [dB]** | 5 |
| **Additional Losses [dB]** | 1 |
| **Shadow Fading Margin (for std=4dB) @ 95% [dB]** | 0 |

Table 4.5: Downlink budget parameters.

In the downlink transmission, in order to achieve the highest possible spectral efficiency, it is needed a minimum EIRP of 47 dBW for a LEO satellite at 600 km altitude. Due to the NB-IoT system limitations, having a higher EIRP at the satellite does not give any improvement in terms of spectral efficiency. In fact, the link can be closed with lower EIRP values but reducing the spectral efficiency.

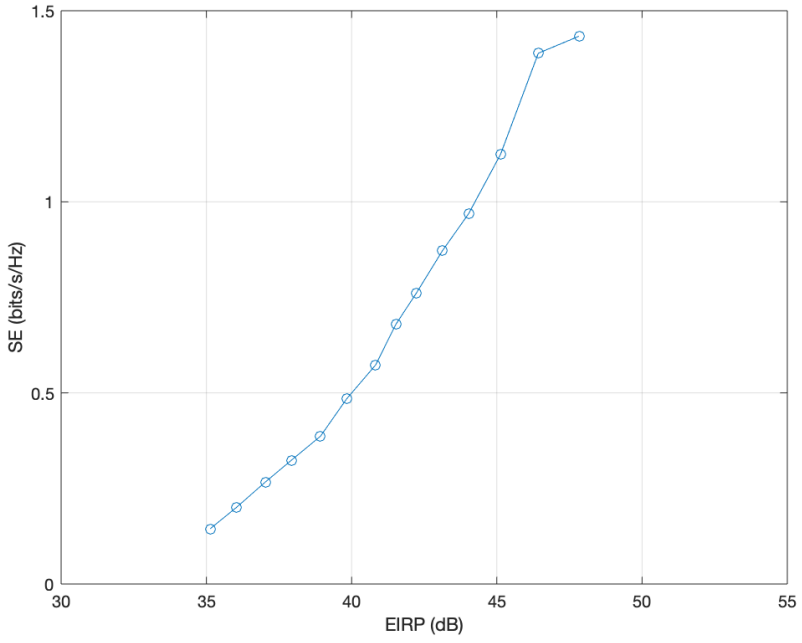


Figure 4.6: Link budget result for downlink transmission between a NB-IoT device and a LEO satellite.

It is important to highlight that the additional losses might be also the ones related to line implementation losses which are mainly caused by RF coupling losses, pointing and beamforming errors, and any other source related to miniaturization and assembling issues.

Last but not least, an important feature of NB-IoT system is that devices can send the information again in case the flying-gNB does not demodulate correctly, which increases the availability of the information.

## 4.4 Channel Estimation

Another important aspect regarding the implementation of a direct link between a NB-IoT are the phase and amplitude fluctuations which determine the channel stationary time. In satellite communications, the Doppler spread $\Delta f_d$ (i.e. the width of the Doppler spectrum) is about the 10% of the Doppler frequency. Given the minimum satellite elevation angle $\theta_{UE} = 40°$, the corresponding Doppler shift is 353.2 kHz (see Table 3.3). Then, the Doppler spread $\Delta f_d$ can be computed as follows:

$$\Delta f_d = f_d \cdot 0.1 = 353.2\,\text{kHz} \cdot 0.1 = 35.32\,\text{kHz} \tag{4.5}$$

The stationary time $t_s$ is inversely proportional to the Doppler spread. Therefore, can be calculated as follows:

$$t_s = \frac{1}{\Delta f_d} = \frac{1}{35.32\,\text{kHz}} = 28.31\,\mu\text{s} \tag{4.6}$$

As it can be observed, this will lead to a challenging scenario, mainly because the stationary time $t_s$ is lower than the symbol duration $T_u = 66.7\,\mu$s corresponding to the SCS $\Delta f = 15\,$kHz. Higher SCS values will allow to correctly estimate the channel, but current NB-IoT system only supports SCS of 3.75 or 15 kHz. Since the channel should be estimated much more often than the stationary time, given the Doppler shifts of the current scenario and the SCS supported by the NB-IoT system, it will not be possible to correctly estimate the channel. Notice that to obtain a stationary time $t_s$ approximately equals to the symbol duration $T_u = 66.7\,\mu$s a minimum elevation angle $\theta_{UE} = 70°$ will be needed. Therefore, it can be stated that Doppler compensation methods are needed for this type of scenarios.

In Chapter 5 a time diversity beamformer for reception in grant-free access will be described [7]. The main advantage is that the proposed access technique does not require channel estimation or prior network scheduling and provides benefits in terms of probability of collision.

## 4.5 Signal Model

First, the modelling of the channel will be formulated. The LEO satellite communication channel can be characterized in two parts, the first due to the scattering and the obstacles around the

NB-IoT devices and the second due to the change of the frequency of the signal (i.e. Doppler shift). Given the satellite propagation model ITU-R M.1225 Channel Model C described in Table 4.2, which is the one implemented in this work, the Channel Impulse Response (CIR) can be formulated as:

$$h(t,\tau) = \left(\sqrt{\mathrm{P_{LOS}}} + h_0(t)\right)\delta(t) + \sum_{l=1}^{L-1} h_l(t)\delta(\tau - \tau_l) \tag{4.7}$$

where $L$ are the number of taps. In case $L > 1$ the transmitted signal will travel over different paths with respect to the first tap, meaning that the channel is frequency selective (FS) and intersymbol interference (ISI) will be expected. It will be assumed that the taps will be located at different times and positions with respect to the first one, being the first tap corresponding to the shortest path from the NB-IoT device and the LEO satellite and assumed to be in LOS conditions.

In addition, Doppler shift due to satellite motion should be taken into account according to the equation 3.8. This additional Doppler shift should be applied to all the taps, and it will be assumed to be constant during the symbol time. Then, the CIR can be reformulated as:

$$h(t,\tau) = \exp(j2\pi f_d t + j\theta_0)\left(\left(\sqrt{\mathrm{P_{LOS}}} + h_0(t)\right)\delta(t) + \sum_{l=1}^{L-1} h_l(t)\delta(\tau - \tau_l)\right) \tag{4.8}$$

Considering the uplink physical channel with $N_d$ NB-IoT devices, each one transmitting a SC-FDMA signal, the samples of a given SC-FDMA symbol of device "$i$" can be denoted by vector $\boldsymbol{x}_i(n) = [x_i(n)\, x_i(n-1) \cdots x_i(n-L_i+1)] \in \mathbb{C}^{L_i \times 1}$, and the channel taps can be denoted by vector $\boldsymbol{h}_i = [h_{i,0}\, h_{i,1} \cdots h_{i,L_i-1}] \in \mathbb{C}^{L_i \times 1}$ for $i = 1, 2, ..., N_d$.

Therefore, the signal that is collected at the antennas of the LEO satellite (i.e. flying-gNB) given by $\boldsymbol{y}(n) \in \mathbb{C}^{N_a \times 1}$, where $N_a$ is the number of antennas of the LEO satellite, can be expressed as follows:

$$\begin{aligned} \boldsymbol{y}(n) &= \sum_{i=1}^{N_d} \boldsymbol{S}_{\boldsymbol{h}_i} \boldsymbol{h}_i^* \circ \boldsymbol{x}_i(n) + \boldsymbol{n} = \sum_{i=1}^{N_d} [\boldsymbol{s}_{h_{i,0}}\, \boldsymbol{s}_{h_{i,1}} \cdots \boldsymbol{s}_{h_{i,L_i-1}}]\, \boldsymbol{h}_i^* \circ \boldsymbol{x}_i(n) + \boldsymbol{n} = \\ &= \sum_{i=1}^{N_d} \left( h_{i,0}^* x(n) \boldsymbol{s}_{h_{i,0}} + h_{i,1}^* x(n-1) \boldsymbol{s}_{h_{i,1}} + \cdots + h_{i,L-1}^* x(n-L+1) \boldsymbol{s}_{h_{i,L-1}} \right) + \boldsymbol{n} \end{aligned} \tag{4.9}$$

where $\circ$ denotes the Hadamard product and $\boldsymbol{s}_{h_{i,l}} \in \mathbb{C}^{N_a \times 1}$ stands for the steering vector of device "$i$" coming from the angle associated with the respective multipath of the channel. Compacting all the steerings from a NB-IoT device, the matrix $\boldsymbol{S}_{\boldsymbol{h}_i} \in \mathbb{C}^{N_a \times L_i}$ is obtained. In general, a steering vector of a planar array whose direction of arrival (DOA) is given by ($\theta_s$,$\varphi_s$) is formulated as: $\boldsymbol{s}(\theta_s, \varphi_s) = [1\, e^{-2\pi \frac{f_c}{c} D \sin(\theta_s)\cos(\varphi_s - \varphi_q)}\, e^{-2\pi \frac{f_c}{c} 2D \sin(\theta_s)\cos(\varphi_s - \varphi_q)} \cdots e^{-2\pi \frac{f_c}{c} (N_a - 1) D \sin(\theta_s)\cos(\varphi_s - \varphi_q)}]$, where $D$ represents the distance between antennas, which is designed as $\frac{\lambda}{2}$, $f_c$ is the carrier frequency and $c$ is the speed of light. Th Additive White Gaussian Noise (AWGN) found at the receiver is represented as $\boldsymbol{n} \sim N(0, N_o I) \in \mathbb{C}^{N_a \times 1}$. As the formulation presented in this section corresponds a general case of a channel with multipath, the steering vector is the one with the DOA corresponding to the stronger arriving array.

In the case of the scenario presented in this work, the coherence bandwidth of the LEO satellite channel can be calculated as follows [6]:

$$BW_c = \frac{1}{5\,T_m} = \frac{1}{5 \cdot 25\,n\text{s}} = 8\,\text{MHz} \tag{4.10}$$

where $T_m$ is the maximum delay spread. It can be observed that the bandwidth of the LEO Sat-IoT system (i.e. 180 kHz) is considerably less than $BW_c$, then the channel can be considered flat. This means that a single channel tap is sufficient to represent the satellite channel.

# Chapter 5

# Smart Beamforming for 5G

## 5.1 Resource Sharing Beamforming Access (RSBA)

The proposed RSBA is based in a Grant-Free access and its goal is to reduce the probability of collision in NOMA without increasing signaling overhead or the UE complexity while taking advantage of the spatial dimension. In NOMA, users can use the same non-orthogonal resources (e.g. same subcarriers) and thus achieving higher spectral efficiency. For this scenario, one type of Signature-Based NOMA (S-NOMA) is implemented. In particular, it will be assumed that NB-IoT devices will make use of the Repetition Division Multiple Access (RDMA). This signature-based scheme employs different cyclic-shift repetition patterns at the symbol-level to design device-specific signatures, providing both time and frequency diversity. In fact, this is an advantage in order to create blind beamformers (i.e. without the need of any additional pilot or training sequences) thanks to the redundancy that RDMA presents.

Current wireless systems such as 4G-LTE are not designed to support massive connectivity with a large number of devices. In fact, in LTE, scheduling is required to establish a connection between the gNB and the NB-IoT device. This scheduling encompasses different steps, starting from requesting resources, then waiting for the acknowledgment and finally starts transmitting the information. However, in the context of massive connectivity, this procedure has many drawbacks. On the one hand, small data bursts (i.e. short packet transmissions) will lead to signaling overhead and low spectrum efficiency. On the other hand, in addition to the propagation delay caused by the distance between the NB-IoT devices and the LEO satellite, extra round-trip delay by scheduling will provoke large delays, which is critical in this type of scenarios.

Therefore, the proposed GF S-NOMA is well suited for IoT scenarios (e.g. precision agriculture) where sporadic small data bursts are transmitted. To deal with the scheduling procedure, the GF access allows NB-IoT devices transmitting without waiting for a grant. In this case, the NB-IoT devices will transmit a pilot sequence (or preamble) and data at the same time (see Fig. 5.1).

This type of access provides much shorter access delay, which is suitable in the scenario presented in this work, and reduces the amount of signaling. However, in the case of massive access, it is required to deal with the collisions between NB-IoT devices when they are trying to get the same frequency resources at the same time and with the same repetition patter. As a solution, it is proposed to spatially separate users via smart beamforming.

For the uplink, in the NB-IoT system, the two physical channels NPUSCH and NPRACH, and the DMRS are defined. Despite the proposed beamformer does not require any training sequence, it is needed to embed the NPRACH in order to transmit a random access preamble from the NB-IoT device to indicate to the flying-gNB a random-access attempt and to assist the LEO satellite to adjust the uplink timing of the NB-IoT device, among others parameters. In addition, the DMRS has to be embedded so the LEO satellite will be able to produce channel estimates for demodulation of the associated physical channel.

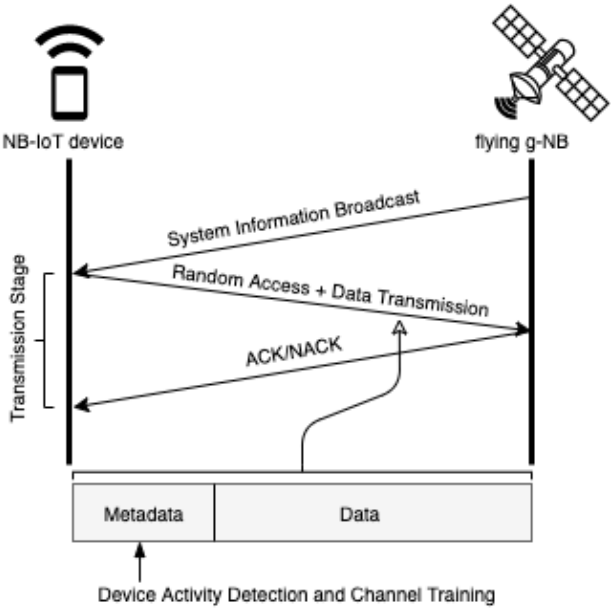


Figure 5.1: GF Access Procedure between a NB-IoT device and a LEO satellite.

Note that, in the GF access, NB-IoT signature for activity detection (NPRACH), channel training (DMRS) and information data are sent in the same packet or frame.

Given the frame structure presented in Fig. 5.2, which it will be defined for the RSBA scheme, each NB-IoT device will repeat a training sequence at two different positions. Note that this sequence value do not need to be known by the flying-gNB, the only requirement for the gNB is to know where the training can be allocated in order to design the beamformer. As training sequences it is proposed to employ Zadoff-Chu (ZC) sequences. In fact, these are the ones used in the contention-based access scheme in LTE and NB-IoT. These sequences are used due to their good properties such as constant amplitude before and after DFT, zero cyclic auto-correlation and

low cross-correlation.

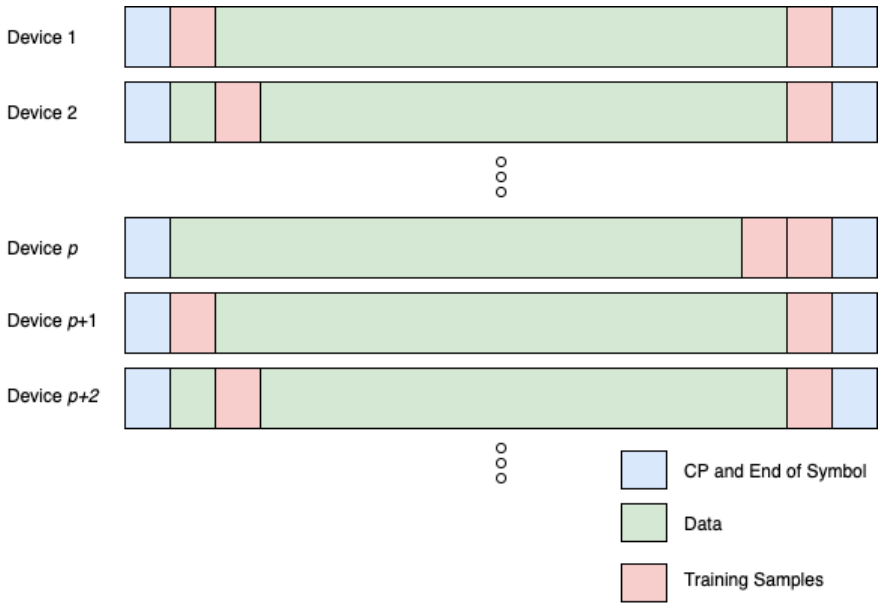


Figure 5.2: Frame structure for the RSBA scheme, where each device repeats in a particular time slot its training sequence.

Then, with the proposed repetition pattern Fig. 5.2 and thanks to the knowledge of the receiver about where the training could be located, a beamformer $\mathbf{b}_i$ can be designed for each NB-IoT device "$i$", such that the following quadratic cost function is minimized:

$$\min_{\mathbf{b}_i} \quad \mathbb{E}\left\{|\mathbf{b}_i^H\mathbf{x}_1 - \mathbf{b}_i^H\mathbf{x}_2|^2\right\} \tag{5.1}$$

$$\text{s.t.} \quad 2\,\Re\left\{\mathbb{E}\left\{\mathbf{b}_i^H\mathbf{x}_1\mathbf{x}_2^H\mathbf{b}_i\right\}\right\} = \gamma \tag{5.1a}$$

where $\mathbf{x}_1$ and $\mathbf{x}_2$ refer to the first and second block of the repeated symbols, respectively. The LEO satellite (i.e. flying gNB) will receive a combination of all the NB-IoT devices frames, and in order to create a combiner for a particular device, it will need the first part of the training (which it can be variable inside the imaginary grid), $\mathbf{x}_1$, and the second part of the training (fixed at the end of the frames for all the devices), $\mathbf{x}_2$. The constraint (Eq. (5.1a)) avoids the undesired solution, being the null vector, where $\gamma$ is a constant different from zero. Also, note that this constraint takes into account that both snapshots are correlated, which is true since they share training.

Therefore, defining $\mathbf{R}_{kl}$=$\mathbb{E}\left\{\mathbf{x}_k\mathbf{x}_l^H\right\}\forall\, k,l = 1,2$, the solution to such problem is:

$$(\mathbf{R}_{11} + \mathbf{R}_{22})\mathbf{b}_i = (1+\lambda)(\mathbf{R}_{12} + \mathbf{R}_{12}^H)\mathbf{b}_i \tag{5.2}$$

$i$ = 1,2, ..., $N_d$, where $\lambda$ is the Lagrange multiplier. Given a particular scenario, in the first set of snapshots $\mathbf{x}_1$, the training of the source of interest (i.e. the source that gNB will be interested to point) and the data from the rest of devices will be found. While in the second set of snapshots $\mathbf{x}_2$,

the training sequences of all devices will be found, as it can be observed in Fig. 5.2. Then, given the proposed beamformer, the preserved signal is the one from the direction of the device that sends the same in both $\mathbf{x}_1$ and $\mathbf{x}_2$. In addition, at the output of such beamformer, the directions from which arrives power from other devices will be nulled.

Given a scenario where sources (i.e. NB-IoT devices) are located at different elevation angles $[-30° - 20° \, 0° \, 30°]$ using $N_a = 49$ (7x7) and a SNR = 6.9 dB. The beamformer (see Fig. 5.3) will point to the source where the selected $\mathbf{x}_1$ only contains training from a particular device and data from the rest, and $\mathbf{x}_2$, as mentioned before, will contain the training from all of the devices. As it can be observed, the training will correspond to the device located at 30°, and thus, the beamformer only points to this device and nulls the rest.

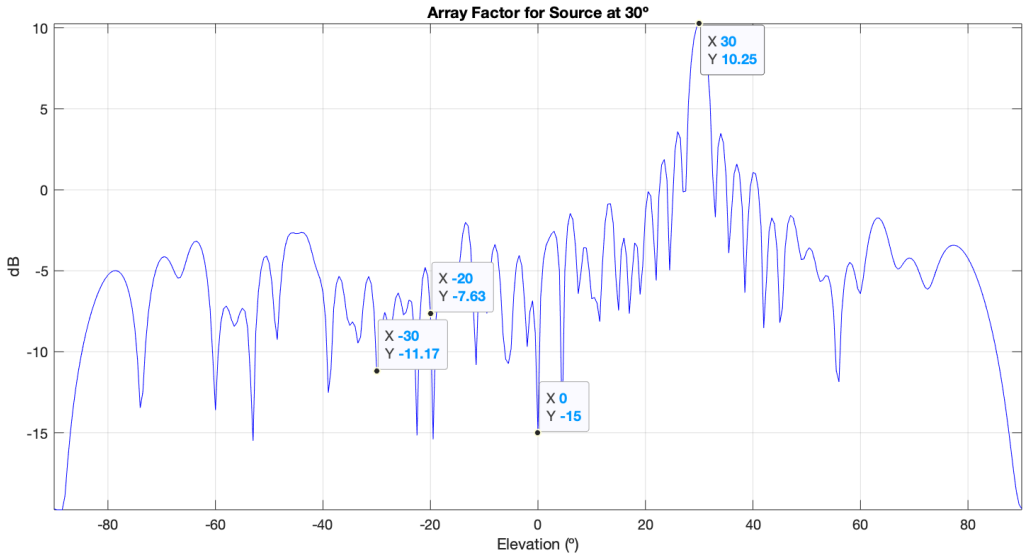


Figure 5.3: Array response for the source of interest located at 30°. The rest of the sources are nulled. The flying-gNB is taking snapshots $\mathbf{x}_1$ and $\mathbf{x}_2$ at the frame positions where the source located at 30° is allocating its training.

However, it can be possible that more than one device transmits its pilot (or training sequence) in the same training slot $\mathbf{x}_1$, and thus, have the same repetition pattern. Figure 5.4 described this situation, in this case, two sources located at $[-30° \, 30°]$ have transmitted its training at $\mathbf{x}_1$ while the other sources located at $[-15° \, 0°]$ have transmitted part of its data. This situation will lead the combiner to point to more than one device.

One might think that employing different ZC sequences will help to distinguish the devices, however, this beamformer is designed in such a way that distinguishes the devices by their different repetition patters in time without the need of knowing the value of these sequences. Then, using same or

different ZC sequences will not have an impact in the beamformer.

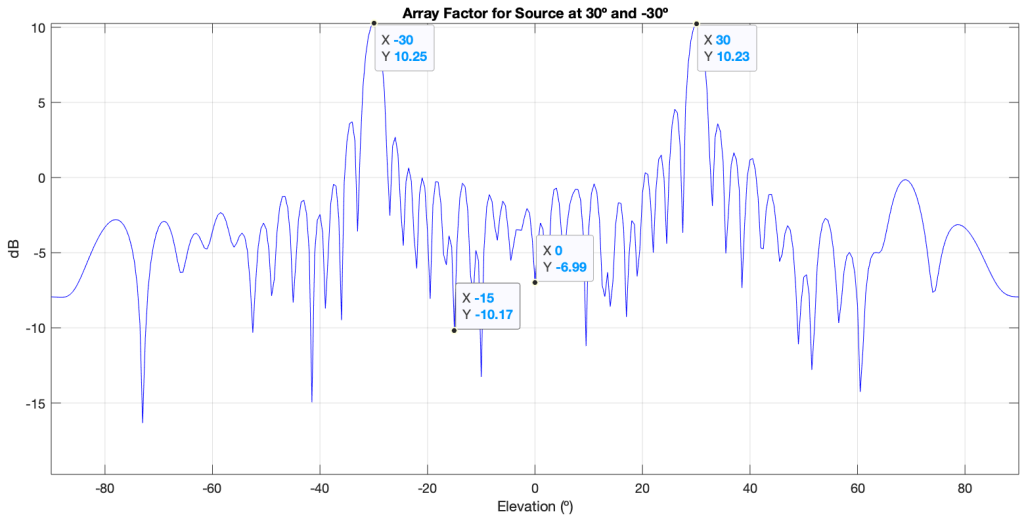


Figure 5.4: Array response for the sources that are sharing training located at 30° and −30°.

Even in the scenarios where the snapshot $\mathbf{x}_1$ contains training sequences from more than one device, thanks to the large number of antennas that the flying-gNB can have in mm-waves, the sources will be spatially identified with high resolution. And thus, will allow the LEO satellite to correctly estimate the DOA of each device transmitting in that moment. After this DOA estimation stage, the steering vector of each device "$i$" is known, $\mathbf{s}_i$, and then different spatial reference beamformers can be applied. The architecture presented in this work (see Fig.2.2) employs a phased array beamformer, defined as $\mathbf{b}_{i,s} = \mathbf{s}_i$, where subindex "$s$" refers to separate. Note that DOA estimation with phased array is what NR proposes under the beam sweeping mechanism in order to support beamforming for initial access [6]. In addition, assuming that devices will be under LOS conditions, multipath could be negligible, and this will simplify the equalizer that must be placed at the receiver to make a correct demodulation. If multipath is present, different signal replicas of the same device could be received at the flying-gNB and this will lead to generate additional false DOAs within the beamformer.

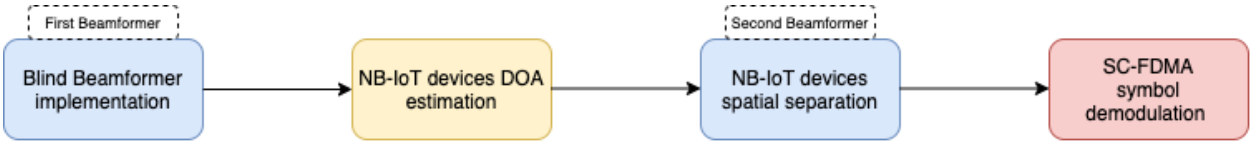


Figure 5.5: Block diagram with the steps needed at the LEO satellite to implement the proposed RSBA scheme to point device by device.

As presented in the block diagram (see Fig.5.5), the proposed RSBA consists in the following steps: (i) Blind beamforming; (ii) NB-IoT devices DOA estimation by identifying the maxima of the blind beamformer; (iii) Form a dedicated beam towards each identified DOA; (iv) For each NB-IoT device, the channel can be subsequently estimated and the information demodulated.

## 5.2 NB-IoT Devices Collision Analysis

In this section, the gain in terms of probability of collision that the proposed RSBA provides will be discussed. First, let's consider a GF-MA scenario where different devices are trying to get resources and spatial separation has not been applied (i.e. no beamforming). In this scenario, devices will directly pick any of the available subcarriers (with no prior scheduling) to transmit data. Hence, it can be assumed that a collision will occur if any of the devices tries to get the same frequency resources at the same time and with the same repetition pattern. This probability of collision without using the aforementioned RSBA technique can be denoted as $P_{C,RD}$.

As it will be observed in this section, this probability $P_{C,RD}$ depends on different parameters, such as the number of active devices, $N_d$, the bandwidth associated to each device or type of NB-IoT transmission (e.g. SC, MT-6, MT-12), and the type of NOMA detector (i.e. single user detector - SUD or, sequential interference canceller - SIC). For the case that the LEO satellite implements SUD for each device, the $P_{C,RD}$ coincides with the probability that devices collide in time and frequency.

In addition, the probability of collision without beamforming depends on the length of the training sequences, which employ Zadoff-Chu (ZC) sequences. The longer the sequences, the less probability of collision between the devices will be. The problem of using very long sequences to reduce the probability of collision is that they will not be orthogonal and thus, this will increase the probability of error in the detection of the information since it has to be done with interference from other sequences.

However, the proposed RSBA scheme via smart beamforming solves the trade-off between better orthogonality and larger sequence space. In [24], instead of employing ZC sequences, it is proposed to use second-order Reed-Muller (RM) codes for grant-free massive access in 5G NR. These RM sequences have many features that make them interesting: (i) it can create a sequence space of orders of magnitudes larger than ZC with same-length sequences, (ii) in both small-sized and large-sized sequence spaces, the detection can be much faster than of ZC sequences. For the beamformer design that is proposed, any training sequence with the mentioned properties in can be used, as long as it meets that its correlation with the data is zero.

Even thought S-NOMA is a good solution to deal with massive scenarios, such architectures do not contemplate using the signature to separate the devices in space, which is the purpose of RSBA. Taking advantage of the different repetition patters in time assigned to each device, spatial

separation will be implemented (i.e. RSBA). Therefore, if devices are spatially separated, $P_{C,RD}$ will not be a problem as the beamformer would separate the colliding signals, and thus, it will decrease $P_{C,RD}$. As the flying-gNB is able to point device by device, in case two or more devices send information at the same frequencies, the spatial processor will only allows the one at which is pointing.

In addition to $P_{C,RD}$, a probability of collision in the spatial domain has to be defined, which corresponds a measure of the number of wrong detected sources by the RSBA, $P_{C,S}$ . It is important to highlight this probability of collision because it directly depends on the LEO satellite antenna array size. In the case of an omnidirectional spatial response (e.g. $N_a$=1), there will be only one beam covering all possible angles, and thus, it will not be possible to differentiate the devices in space. However, mm-waves (e.g. Ka-Band) will allow the LEO satellite to employ a large number of antennas, and thus, a higher resolution will be achieved. This resolution will allow the flying-gNB to correctly detect the position of the active devices. Finally, the total probability of collision for the RSBA scheme, combining frequency and space, is given by:

$$P_{C,RS} = P_{C,RD} \cdot P_{C,S} \tag{5.3}$$

For this section, due to the hight computational cost of running massive scenarios, a maximum number of $N_d$= 120 devices has been considered. These devices are located at different positions, at a minimum elevation angle $\theta_{UE}$=40° towards the LEO satellite, and $-45° \leq \varphi_s \leq 45°$. Four different scenarios have been defined, where devices request different number of subcarriers and different total number of subcarriers are available. In addition, different antenna sizes have been considered $N_a$ = [256 324 400] with a distance between antenna elements of $\frac{\lambda}{2}$.

Table 5.1 describes the configurations for the different scenarios. For instance, the proposed scenarios can be deployed in the aforementioned exclusive satellite band of 500 MHz between 19.7 GHz and 20.2 GHz.

| | **Scenario (a)** | **Scenario (b)** | **Scenario (c)** | **Scenario (d)** |
|---|---|---|---|---|
| **Channel Model** | Ricean (LOS) | Ricean (LOS) | Ricean (LOS) | Ricean (LOS) |
| **NB-IoT Transmission Mode** | MT-12 | MT-6 | MT-12 | MT-6 |
| **# Total Available Subcarriers** | 601 | 601 | 301 | 301 |
| **# Requested Subcarriers** | 12 | 6 | 12 | 6 |
| **SNR [dB]** | 6.9 | 6.9 | 6.9 | 6.9 |
| **Spectral Efficiency [b/s/Hz]** | 1.43 | 1.43 | 1.43 | 1.43 |
| **Minimum LEO G/T [dB/K]** | 21 | 18 | 21 | 18 |

Table 5.1: Definition of the proposed scenarios.

The first two scenarios have a total number of available subcarriers of 601. In scenario (a) (see Fig.5.6), the type of transmission is MT-12, that means that each of the devices randomly requests 12 subcarriers among the 601 available. As it can be observed, the use of a spatial processor to distinguish the devices reduces the probability of collision. Besides, at it is expected, the total probability of collision of the RSBA scheme will increase when the number of devices accessing to the media increases. In this case, to obtain a SNR = 6.9 dB and achieve the highest spectral efficiency allowed, a minimum G/T of 21 dB/K at the LEO satellite will be needed.

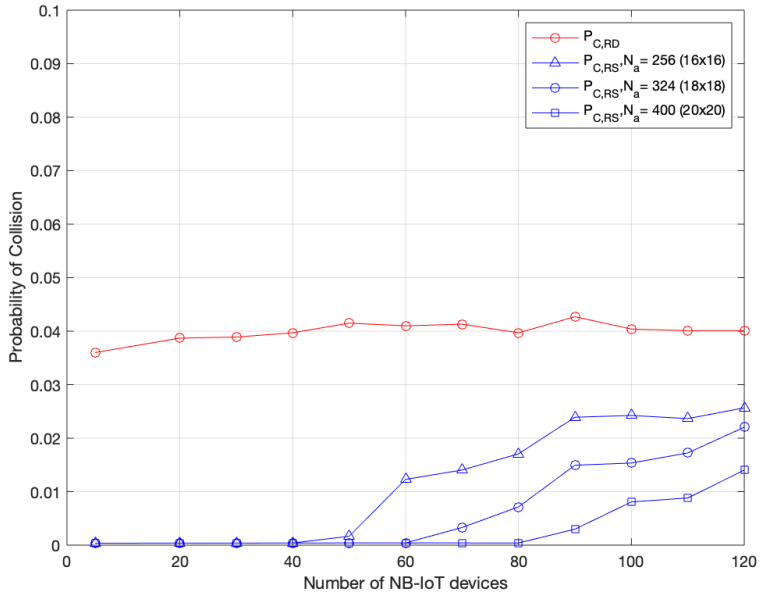


Figure 5.6: Probability of collision without (red) and with (blue) spatial diversity for the scenario (a) with different antenna arrays configurations.

In scenario (b) (see Fig.5.7), the probability of collision $P_{C,RD}$ will decrease because is less probable that active devices get the same resources as they are randomly requesting 6 subcarriers instead of 12. In this case, to obtain a SNR = 6.9 dB and achieve the highest spectral efficiency, a minimum G/T of 18 dB/K at the LEO satellite will be needed. Note that this value corresponds for devices located at $\theta_{UE} = 40°$, which is the minimum elevation angle considered in these scenarios. As it will be observed in the different scenarios, the more antennas the LEO satellite have, the narrower the beams will be, and better performance will be achieved. That means if there are two or more active devices very close, the beamformer could distinguish them.

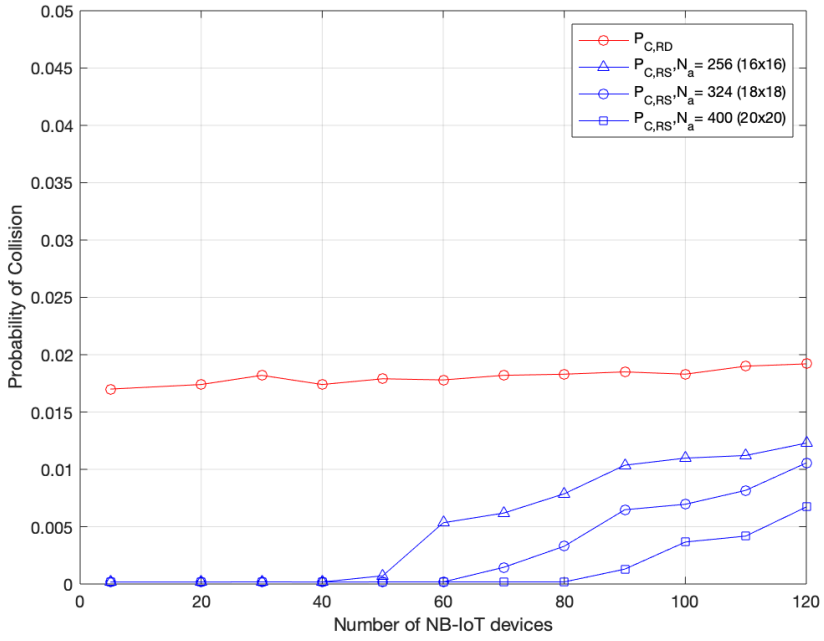


Figure 5.7: Probability of collision without (red) and with (blue) spatial diversity for the scenario (b) with different antenna array configurations.

In the last two scenarios, the total number of available subcarriers are 301. If the scenario (a) is compared with the scenario (c) (see Fig.5.8), it can be seen that if the mode of transmission is the same (MT-12), the probability of collision will be higher due to less subcarriers are available. The same will happen if the scenario (b) is compared with scenario (d) (see Fig.5.9). Note that in all the scenarios, a SCS of 15 kHz for data transmission has been considered. It is important to highlight that other scenarios could be considered, such as the ones where the number of available subcarriers is lower. In these cases, other type of transmissions could be considered, such as ST with SCS of 3.75 kHZ. Therefore, lower G/T at the LEO satellite will be required (nearly 5 dB/K). However, as it mentioned in the previous chapter, choosing one transmission mode or another it will impact the whole NB-IoT system, including important aspects such as delay, capacity, and energy consumption.

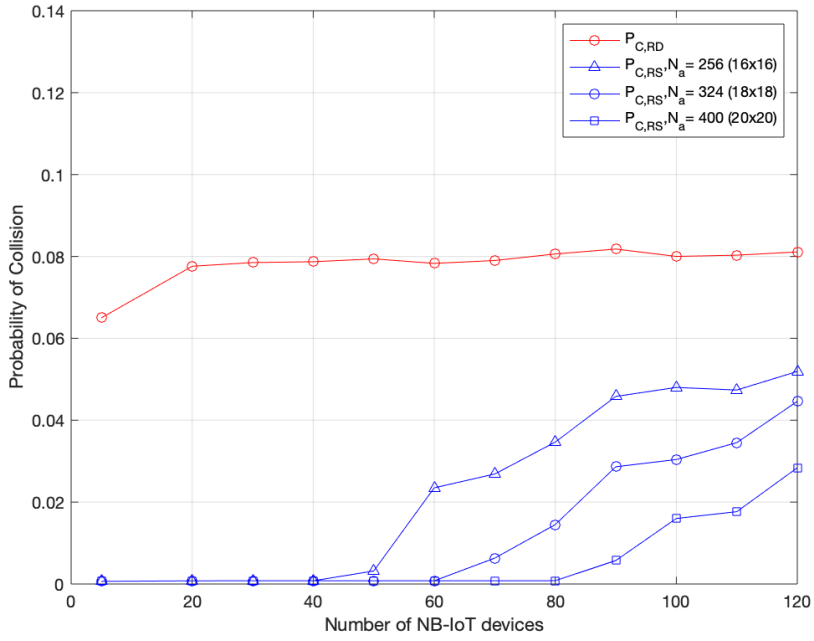


Figure 5.8: Probability of collision without (red) and with (blue) spatial diversity for the scenario (c) with different antenna array configurations.

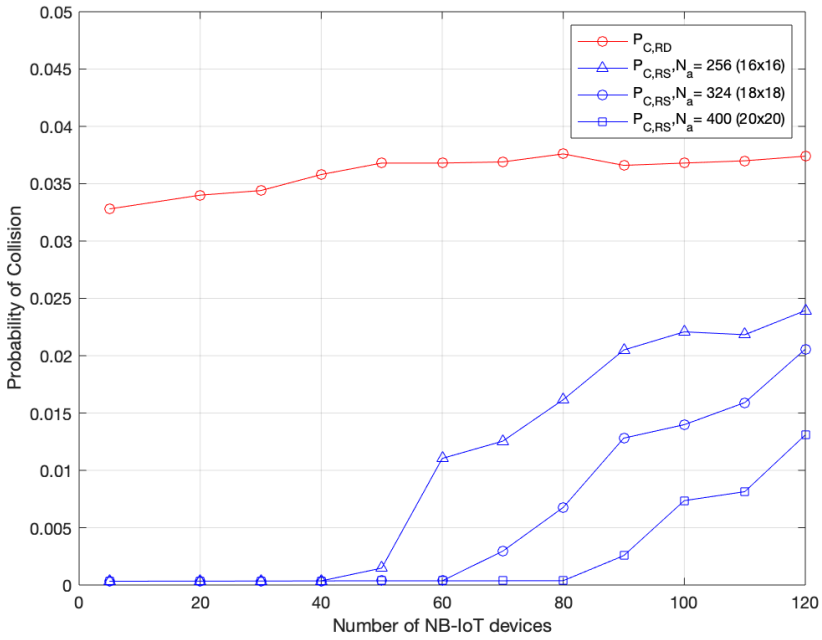


Figure 5.9: Probability of collision without (red) and with (blue) spatial diversity for the scenario (d) with different antenna array configurations.

# Chapter 6

# Conclusions

Providing worldwide coverage is nowadays a challenge, and satellite communications provides stands out as a promising candidate. During this project, a possible system architecture to deal with massive scenarios is proposed. As it is explained in the project, establishing a direct link between a LEO Satellite and a NB-IoT poses severe challenges such as delay, satellite coverage, and Doppler shifts. Chapter 3 contains a full explanation of these aspects, particularly for a LEO satellite (at an height of 600 km) operating at Ka-Band (20 GHz). In fact, one of the most critical problems is the Doppler shift. The considerable difference between the terrestrial and non-terrestrial Doppler shifts requires to employ compensation methods mainly because is not tolerated by the current 5G NR standard. Then, as it is proposed, GNSS systems seems to be a suitable solution to compensate these Doppler shifts and also for providing useful information such as the actual position of the satellite and the UE. In Chapter 4, technical challenges regarding 5G NR are presented, and in particular for the physical layer. Since NB-IoT system allows to employ different modes of transmissions, the link budget for each of the cases has been studied. This led to obtain useful information such as the required G/T at the LEO satellites, which has to be carefully designed before launching new satellites to support NB-IoT services.

Finally, considering that 5G NR is the first generation of wireless standard that considers the spatial dimension in a feasible and practical way, this work has proposed to incorporate this spatial dimension to current NOMA schemes. In Chapter 5, a way to distinguish sources even if they transmit in the same frequency has been presented. In addition, due to the large number of devices present in massive scenarios, pointing devices on by one is needed. Therefore, a second beamformer has been implemented. Summarizing, this work showed that the implementation of such beamformers, firstly a blind beamformer to detect the sources, and secondly phased array beamformers to form dedicated beams towards each identified DOA, allow to decrease the probability of collision taking advantage from the spatial subspace using the RDMA scheme. It is expected that this work provides useful information for the development of LEO satellite systems, and in particular for NB-IoT massive scenarios in 5G NR at mm-waves.

Future research lines could be the study of this scenario with other type of UEs, such as very small aperture terminals, where the transmitted power and the antenna gain are higher. Further possible studies include the understanding of how the shadowing and multipath behaves in various environments (e.g. urban, suburban, and tree shadowed). Also, it will be interesting to study how spatial diversity could improve other S-NOMA schemes (e.g. schemes based on code sequences and/or patterns). Another important point is to study what will happen if devices are non-static and how it will impact to the scenario presented in this work.

# Appendices

# Appendix A

# Work Plan

## A.1 Work Packages, Tasks and Milestones

The work packages of the project are the following:

- **WP1** - Definition of Project Tasks: Define the main goals and objectives of the project. The starting date was 17/02/2020 and the end date was 26/02/2020.
- **WP2** - System Architecture: Study of the current NTN architectures and how could be adapted to a massive IoT scenario. The starting date was 26/02/2020 and the end date was 26/03/2020.
- **WP3** - LEO Satellite Characterization: Assessment of the channel impairments of a direct access between a NB-IoT device and a LEO satellite. The starting date was 26/03/2020 and the end date was 26/04/2020.
- **WP4** - 5G NR Physical Layer Challenges: Study of different aspects regarding 5G NR, also includes link budget performance studies. The starting date was 26/04/2020 and the end date was 30/06/2020.
- **WP5** - Smart Beamforming implementation and simulation results: Assessment of the proposed RSBA scheme and simulate the performance. The starting date was 30/06/2020 and the end date was 10/08/2020.
- **WP6** - Project writing: Write of the work developed. The starting date was 10/05/2020 and the end date was 17/08/2020.

## A.2 Gantt Diagram

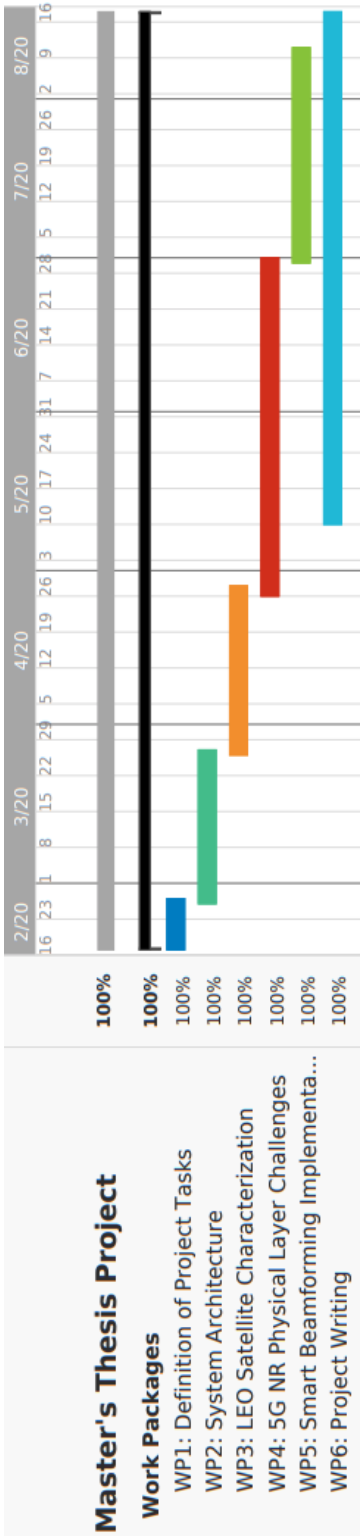


Figure A.1: Gantt Diagram.

# Bibliography


[1] 3GPP, "Study on using Satellite Access in 5G," Technical Report (TR) 22.822, 3rd Generation Partnership Project (3GPP), 06 2018. Version 16.0.0.

[2] 3GPP, "Study on Scenarios and Requirements for Next Generation Access Technologies," Technical Report (TR) 38.913, 3rd Generation Partnership Project (3GPP), 06 2018. Version 15.0.0.

[3] 3GPP, "NR-NTN work plan," TSG RAN WG1 Meeting nr. 100bis, Busan, Korea, R1-20XXX, 3rd Generation Partnership Project (3GPP), 04 2020.

[4] P. Arapoglou, S. Cioni, E. Re, and A. Ginesi, "Direct Access to 5G New Radio User Equipment from NGSO Satellites in Millimeter Waves," 03 2020.

[5] A. Ivanov, M. Stoliarenko, A. Savinov, and S. Novichkov, "Physical Layer Representation in LEO Satellite with a Hybrid Multi-Beamforming," in *2019 15th International Wireless Communications Mobile Computing Conference (IWCMC)*, pp. 140–145, 2019.

[6] 3GPP, "Study on New Radio (NR) to support non-terrestrial networks," Technical Report (TR) 38.811, 3rd Generation Partnership Project (3GPP), 10 2019. Version 15.2.0.

[7] C. Diaz-Vilor, A. I. Pérez-Neira, and M. Á. Lagunas, "RSBA-Resource Sharing Beamforming Access for 5G-mMTC," in *Proceedings of Globecom 2019, 9-13 December 2019, Waikoloa, HI, USA.*, Dec. 2019.

[8] A. Guidotti, A. Vanelli-Coralli, M. Conti, S. Andrenacci, S. Chatzinotas, N. Maturo, B. Evans, A. Awoseyila, A. Ugolini, T. Foggi, L. Gaudio, N. Alagha, and S. Cioni, "Architectures and Key Technical Challenges for 5G Systems Incorporating Satellites," *IEEE Transactions on Vehicular Technology*, vol. 68, no. 3, pp. 2624–2639, 2019.

[9] S. Han, C. I, Z. Xu, and C. Rowell, "Large-scale antenna systems with hybrid analog and digital beamforming for millimeter wave 5G," *IEEE Communications Magazine*, vol. 53, no. 1, pp. 186–194, 2015.

[10] J. Zhang, X. Yu, and K. B. Letaief, "Hybrid Beamforming for 5G and Beyond Millimeter-Wave Systems: A Holistic View," 2019.

[11] A. Akaishi, M. Iguchi, K. Hariu, M. Shimada, T. Kuroda, and M. Yajima, "Ka-band Active Phased Array Antenna for WINDS Satellite," 04 2003.

[12] Y. Cailloce, G. Caille, I. Albert, and J. M. Lopez, "A Ka-band direct radiating array providing multiple beams for a satellite multimedia mission," in *Proceedings 2000 IEEE International Conference on Phased Array Systems and Technology (Cat. No.00TH8510)*, pp. 403–406, 2000.

[13] R. N. Simons, "Space-based Ka-band direct radiating phased array antenna architecture for limited field of view," in *2016 IEEE International Symposium on Antennas and Propagation (APSURSI)*, pp. 521–522, 2016.

[14] L. Thao, D. Loc, and N. Tuyen, "Study Comparative of Parabolic and Phased Array Antenna," *VNU Journal of Science: Mathematics - Physics*, vol. 30, no. 3, 2014.

[15] A. D. Panagopoulos, P. M. Arapoglou, and P. G. Cottis, "Satellite communications at KU, KA, and V bands: Propagation impairments and mitigation techniques," *IEEE Communications Surveys Tutorials*, vol. 6, no. 3, pp. 2–14, 2004.

[16] ITU-R Recommendation P.618-13, "Propagation data and prediction methods required for the design of Earth-space telecommunication systems," Geneva, Switzerland, 2017.

[17] ITU-R Recommendation P.840-8, "Attenuation due to clouds and fog," Geneva, Switzerland, 2019.

[18] ITU-R Recommendation P.676-12, "Attenuation by atmospheric gases and related effects," Geneva, Switzerland, 2019.

[19] Chun Loo and J. S. Butterworth, "Land mobile satellite channel measurements and modeling," *Proceedings of the IEEE*, vol. 86, no. 7, pp. 1442–1463, 1998.

[20] A. Guidotti, A. Vanelli-Coralli, M. Caus, J. Bas, G. Colavolpe, T. Foggi, S. Cioni, A. Modenini, and D. Tarchi, "Satellite-enabled LTE systems in LEO constellations," in *2017 IEEE International Conference on Communications Workshops (ICC Workshops)*, pp. 876–881, 2017.

[21] M. E. Lutz and A. Jahn, "Satellite Systems for Personal and Broadband Communications," Berlin, Germany, Springer-Verlag, 2000.

[22] 3GPP, "Discussion on link budget for NTN," TSG RAN WG1 Meeting nr. 96bis, Xian, China, R1-1903998, 3rd Generation Partnership Project (3GPP), 04 2019.

[23] O. Kodheli, N. Maturo, S. Andrenacci, S. Chatzinotas, and F. Zimmer, "Link Budget Analysis for Satellite-Based Narrowband IoT Systems," pp. 259–271, 09 2019.

[24] H. Zhang, R. Li, J. Wang, Y. Chen, and Z. Zhang, "Reed-Muller Sequences for 5G Grant-Free Massive Access," in *GLOBECOM 2017 - 2017 IEEE Global Communications Conference*, pp. 1–7, 2017.